INVESTIGATION OF *C/EBPβ* AND *C/EBPδ* EXPRESSION DURING ADIPOGENESIS

Dissertation submitted to the University of Kerala in partial fulfilment of the requirement for the award of the degree of

MASTER OF SCIENCE IN BIOCHEMISTRY

Submitted by

RESHMI R.

Candidate code: 63824142009

Exam code: 63822403

Subject code: BC 544

Under the Guidance of

Prof. (Dr.) R. Rajalakshmi & Dr. Lekshmi N.

Inter University-Centre for Genomics & Gene Technology (IU-CGGT)

University of Kerala, Kariavattom, Thiruvananthapuram



DEPARTMENT OF BIOCHEMISTRY

T. K. M. COLLEGE OF ARTS AND SCIENCE, KARICODE, KOLLAM

JULY 2026

Department of Biochemistry
T.K.M. College of Arts and Science
(Affiliated to University of Kerala)
Re-accredited by NAAC with "A++" Grade
Kollam – 6G1005, Kerala.
www.tkmcas.ac.in

15/07/2026

CERTIFICATE

This is to certify that the dissertation entitled **Investigation of *C/EBPβ* and *C/EBPδ* Expression during Adipogenesis'** submitted to the University of Kerala in partial fulfilment of the requirements for the award of the degree of Master of Science in Biochemistry, is a record of original research work carried out by **RESHMI R. (Candidate code: 63824142009)** of the Department of Biochemistry, T. K. M. College of Arts and Science, Kollam under the guidance and supervision of **Prof. (Dr.) R. Rajalakshmi** and **Dr Lekshmi N.,** in the Inter University Centre for Genomics and Gene Technology (IU-CGGT), University of Kerala, Kariavattom. It is also certified that no part of this work has been presented for the award of any other degree, diploma, or similar title at any other university.

Dr. Sumayya A. S
Internal Guide

Dr. Ajinza A.
Head of the Department of Biochemistry

Examiners: **1.**

2.

Declaration

I hereby declare that the thesis titled **'Investigation of *C/EBPβ* and *C/EBPδ* Expression during Adipogenesis'** is based on original research work carried out by me under the guidance and supervision of **Prof. (Dr.) R. Rajalakshmi** and **Dr. Lekshmi N.**, in the Inter University Centre for Genomics and Gene Technology (IU-CGGT), University of Kerala. I further declare that no part of this work has been presented for the award of any other degree, diploma, or similar title from any other university.

RESHMI R.

Acknowledgement

I express my sincere gratitude to everyone who supported and encouraged me throughout the successful completion of this dissertation.

First and foremost, I thank **God Almighty** for His blessings, strength, and guidance throughout this endeavour.

I am deeply grateful to **Prof. (Dr.) R. Rajalakshmi,** Hon. Director, Inter University Centre for Genomics and Gene Technology (IU-CGGT), for granting permission and providing the necessary facilities to conduct this study. I sincerely thank my guide, **Dr. Lekshmi N.,** Research Associate, IU-CGGT, for her invaluable guidance, encouragement, and constant support throughout this research.

I extend my heartfelt gratitude to **Prof. (Dr.) M. J. Sheeba**, Principal, T. K. M. College of Arts and Science, Karicode, Kollam, for providing me with the opportunity to undertake this project. I also express my sincere thanks to **Smt. Dr. Ajinza A.**, Head of the Department of Biochemistry, my internal guide **Dr. Sumayya A. S.**, and the faculty members **Dr. Soumya S., Dr. Ansil P. N., and Dr. Harishankar H. S.** for their valuable guidance, constant encouragement, and unwavering support throughout the course of this project.

I sincerely thank **Dr. Nadiya F., Mrs. Arya C. S., Mr. Sajith S. K., Mrs. Mihina B. T.,** and all the research fellows and office staffs of IU-CGGT for their continuous support, cooperation, and assistance during the course of my project.

Finally, I express my heartfelt gratitude to my parents, family, and friends for their constant encouragement, love, and unwavering moral support throughout my study.

RESHMI R.

List of Contents

Chapter	Title	Page No.
	List of Figures	
	List of Tables	
	Abbreviations	
	Abstract	
1	Introduction	1 - 5
2	Review of Literature	6 - 11
3	Aims and Objectives	12
4	Materials and Methods	13 - 26
5	Results	27 - 36
6	Discussion	37 - 38
	Summary and Conclusion	39
	References	40 - 48

List of Figures

Figure	Title	Page No.
1	Schematic representation of the cellular composition of adipose tissue	2
2	Schematic representation of white and brown adipocytes	2
3	Schematic illustration of adipocyte differentiation	4
4	Microscopic image showing the morphology of undifferentiated 3T3-L1 cells	27
5	Micrographs showing progressive accumulation of lipid droplets in 3T3-L1 cell during the course of adipocyte differentiation	28
6	Oil Red O Staining of 3T3-L1 cells during adipocyte differentiation	29
7	Representative images of Oil Red O Staining of differentiated 3T3-L1 cells	30
8	Total RNA isolated from cells at various stages of differentiation	31
9	Representative qPCR amplification and melt curve analysis of the *GAPDH* reference gene used for cDNA quality assessment	32
10	Representative amplification curve demonstrating efficient qPCR amplification	33
11	Melt curve analysis	33
12	Relative fold change in *C/EBPβ* gene expression during adipogenesis, quantified by qPCR using the $2^{-(\Delta\Delta Ct)}$ method	34
13	Relative fold change in *C/EBPδ* gene expression during adipogenesis, quantified by qPCR using the $2^{-(\Delta\Delta Ct)}$ method	36

List of Tables

Table	Title	Page No.
1	Work flow of 3T3-L1 cell differentiation	20
2	Reaction mixture used for cDNA synthesis	23
3	Thermal cycling condition for cDNA synthesis	23
4	Primer sequence used for qRT- PCR	24
5	Reaction mixture used for qRT- PCR	25
6	Thermal cycling condition qRT-PCR (40 cycles)	25
7	Biophotometric analysis of RNA quality and purity	30
8	Relative expression of the *C/EBPβ* gene during adipogenesis, quantified by qPCR using the $2^{-(\Delta\Delta Ct)}$ method	34
9	Relative expression of the *C/EBPδ* gene during adipogenesis, quantified by qPCR using the $2^{-(\Delta\Delta Ct)}$ method	35

Abbreviations

cAMP	Cyclic Adenosine Monophosphate
cDNA	Complementary DNA
C/EBPα	CCAAT/Enhancer-Binding Protein Alpha
C/EBPβ	CCAAT/Enhancer-Binding Protein Beta
C/EBPδ	CCAAT/Enhancer-Binding Protein Delta
CREB	cAMP Response Element-Binding protein
Ct	Cycle Threshold
DEPC	Diethyl Pyrocarbonate
DEX	Dexamethasone
DMEM	Dulbecco's Modified Eagle Medium
DMSO	Dimethyl Sulfoxide
EtBr	Ethidium Bromide
FBS	Fetal Bovine Serum
GAPDH	Glyceraldehyde-3-Phosphate Dehydrogenase
IBMX	3-Isobutyl-1-methylxanthine
MDI	3-Isobutyl-1-methylxanthine, Dexamethasone and Insulin
PBS	Phosphate-Buffered Saline
PPARγ	Peroxisome Proliferator-Activated Receptor Gamma

Abstract

Adipogenesis is a tightly regulated biological process through which preadipocytes differentiate into mature lipid-storing adipocytes. This process is controlled by a coordinated transcriptional cascade in which the early adipogenic transcription factors CCAAT/enhancerbinding protein beta (C/EBPβ) and CCAAT/enhancer-binding protein delta (C/EBPδ) play critical roles by initiating the expression of key adipogenic regulators, including peroxisome proliferator-activated receptor gamma (PPARγ) and C/EBPα. The present study aimed to investigate the temporal gene expression patterns of *C/EBPβ* and *C/EBPδ* during adipogenesis in 3T3-L1 preadipocytes. Adipocyte differentiation was induced using a standard adipogenic differentiation medium, and total RNA was isolated from undifferentiated cells and differentiated cells collected at selected time points during adipogenesis. RNA integrity and purity were assessed prior to complementary DNA (cDNA) synthesis. Quantitative real-time polymerase chain reaction (qRT-PCR) was performed to quantify the relative expression levels of *C/EBPβ* and *C/EBPδ*, and gene expression was analyzed using the $2^{-(\Delta\Delta Ct)}$ method after normalization to a housekeeping gene. The results demonstrated differential expression of both transcription factors during adipocyte differentiation. *C/EBPβ* expression was markedly upregulated during the early phase of adipogenesis and subsequently declined as differentiation progressed, whereas *C/EBPδ* exhibited transient induction during the initial stages, followed by reduced expression in mature adipocytes. These findings were consistent with the established roles of *C/EBPβ* and *C/EBPδ* as early regulators of the adipogenic transcriptional cascade. Overall, the study demonstrated that the coordinated temporal expression of these transcription factors is essential for the initiation and progression of adipocyte differentiation, providing a better understanding of the molecular mechanisms underlying adipogenesis.

Chapter 1

Introduction

Adipogenesis is the biological process through which mesenchymal stem cells differentiate into mature adipocytes, which are specialized cells responsible for the storage of excess energy in the form of lipids. This highly regulated process involves a coordinated sequence of molecular and cellular events that begins with the commitment of mesenchymal precursor cells to the preadipocyte lineage. Although committed preadipocytes retain the capacity to proliferate, they must undergo irreversible cell-cycle arrest before initiating terminal differentiation. This transition is orchestrated by a complex network of transcription factors and signaling pathways that regulate the acquisition of the morphological, metabolic, and endocrine characteristics of mature adipocytes (Gregoire, 2001; Rosen & Spiegelman, 2014).

Over the past 25 years, adipocyte differentiation has been extensively studied for its significant role in the development, growth, and remodeling of adipose tissue. Effective adipogenesis is essential for maintaining energy balance and metabolic health, whereas disruption of this process can lead to obesity, insulin resistance, and various metabolic disorders. Obesity is a chronic metabolic condition characterized by the excessive expansion of adipose tissue through adipocyte hypertrophy (an increase in cell size) and adipocyte hyperplasia (an increase in cell number), and the latter of which may result from enhanced adipogenesis. Dysregulated adipogenesis contributes to adipose tissue dysfunction, leading to altered adipokine secretion, chronic low-grade inflammation, insulin resistance, and an increased risk of metabolic disorders, including type 2 diabetes mellitus, hypertension, and cardiovascular disease (Moller & Flier, 1991; Hotamisligil *et al*., 1993; Ye *et al*., 2022; Di Rocco *et al*., 2024).

Adipose tissue is a specialized form of loose connective tissue that serves as the body's primary energy reservoir by storing triglycerides and releasing fatty acids to meet metabolic demands. Although mature adipocytes constitute approximately one-third of the cellular content of adipose tissue, the remaining cellular population comprises mesenchymal stem cells, preadipocytes, endothelial cells, immune cells, and other stromal cells. This heterogeneous composition confers remarkable plasticity, enabling adipose tissue to undergo growth, remodeling, and metabolic adaptation throughout life (Rosen & MacDougald, 2006). Beyond its role in energy homeostasis,

it functions as an active endocrine organ that secretes adipokines involved in regulating metabolism, immune responses, blood pressure, hemostasis, bone metabolism, and reproductive and thyroid functions (Kershaw & Flier, 2004; Rosen & Spiegelman, 2014).

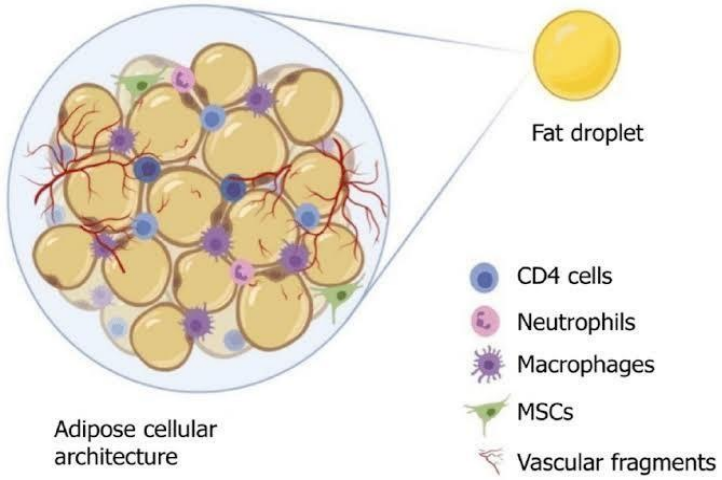


Figure 1. Schematic representation of the cellular composition of adipose tissue (Sharma *et al*., 2021)

Based on its structure and function, adipose tissue is classified into two major types: white adipose tissue (WAT) and brown adipose tissue (BAT). WAT primarily functions as the body's main energy storage site, whereas BAT is specialized for non-shivering thermogenesis through the expression of uncoupling protein-1 (UCP1), thereby increasing energy expenditure and contributing to metabolic regulation (Cannon & Nedergaard, 2004; Wu *et al*., 2012).

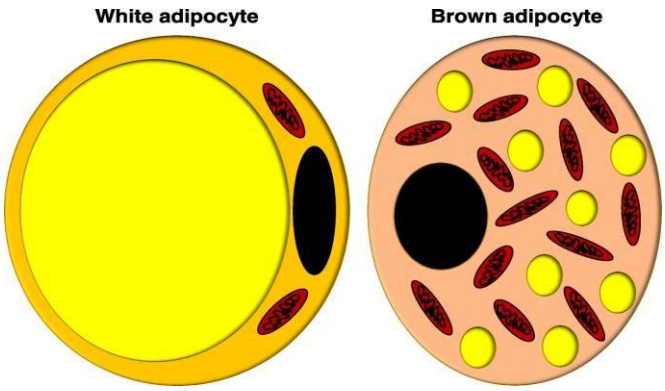


Figure 2. Schematic representation of white and brown adipocytes (Fitzgerald *et al*., 2018)

Unipotent preadipocytes are specialized precursor cells committed to the adipocyte lineage. Under appropriate conditions, they can proliferate and differentiate into mature adipocytes, making them valuable *in vitro* models for investigating adipogenesis. Among the available preadipocyte cell lines, 3T3-L1 and 3T3-F442A are the most widely used, with 3T3-L1 cells considered the goldstandard model for studying white adipogenesis.

Upon differentiation, 3T3-L1 cells undergo growth arrest followed by mitotic clonal expansion, leading to the accumulation of intracellular lipid droplets, increased mitochondrial and endoplasmic reticulum biogenesis, and the sequential activation of adipogenic transcription factors and adipocyte-specific genes involved in lipid metabolism and insulin sensitivity (Green & Kehinde, 1974). During this process, 3T3-L1 cells acquire the morphological and functional characteristics of mature white adipocytes, making them a widely used model for investigating adipocyte biology, obesity, and metabolic disorders (Green & Kehinde, 1974; Novikoff *et al*., 1980; Rosen & Spiegelman, 2014). Furthermore, under specific experimental conditions, these cells exhibit phenotypic plasticity, further expanding their utility in adipose tissue research (Cristancho & Lazar, 2011). These molecular and cellular events closely resemble the adipogenic process *in vivo*, making 3T3-L1 cells a physiologically relevant model for adipogenesis research. Adipocyte maturation is characterized by the upregulation of key lipogenic enzymes, including ATP citrate lyase (ACLY), acetyl-CoA carboxylase (ACC), fatty acid synthase (FASN), malic enzyme 1 (ME1), and stearoyl-CoA desaturase-1 (SCD1), accompanied by increased expression of insulin receptors and glucose transporter type 4 (GLUT4), which together enhance lipid synthesis and insulin responsiveness.

3T3-L1 preadipocytes are routinely cultured in Dulbecco's Modified Eagle Medium (DMEM) supplemented with fetal bovine serum (FBS). Upon reaching confluence, adipogenic differentiation is induced using the MDI cocktail, consisting of insulin, dexamethasone (DEX), and 3-isobutyl-1-methylxanthine (IBMX). Insulin promotes adipogenic signaling through the insulin and insulin-like growth factor-1 (IGF-1) receptors, DEX activates glucocorticoid receptormediated transcription, and IBMX increases intracellular cyclic adenosine monophosphate (cAMP) levels, leading to the activation of protein kinase A (PKA). Together, these factors initiate a coordinated transcriptional cascade that drives adipocyte differentiation and intracellular lipid accumulation (Student *et al*., 1980; Smith *et al*., 1988; Zebisch *et al*., 2012).

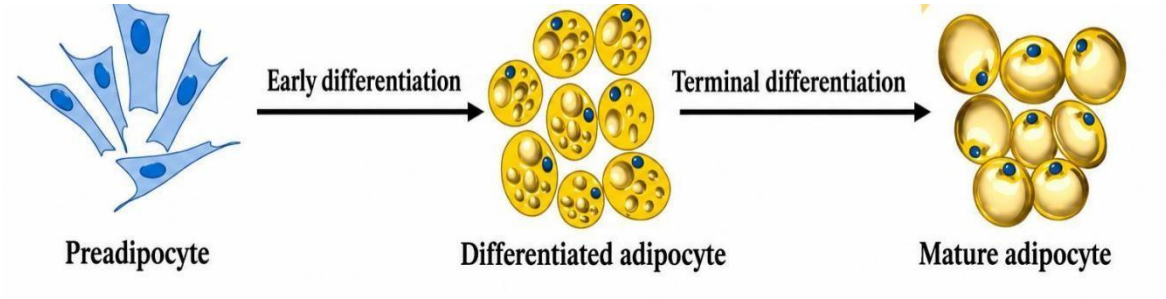


Figure 3. Schematic illustration of adipocyte differentiation (Chularojmontri *et al*., 2022)

Following confluence, 3T3-L1 preadipocytes undergo growth arrest in the G0/G1 phase and acquire adipogenic competence, characterized by the expression of early markers such as lipoprotein lipase (LPL) and type VI collagen (Cornelius *et al*., 1988; Dani *et al*., 1990). During differentiation, preadipocytes undergo marked morphological and molecular changes. Elongated fibroblast-like cells progressively transform into rounded adipocytes with abundant intracellular lipid droplets. This process is accompanied by extracellular matrix (ECM) remodeling and cytoskeletal reorganization, both of which are essential for adipocyte maturation. Proteolytic remodeling of the ECM through the plasminogen activation cascade further facilitates adipocytespecific gene expression and lipid accumulation (Selvarajan *et al*., 2001; Gregoire *et al*., 1998). As differentiation progresses, mature adipocytes express characteristic markers, including fatty acid-binding protein 4 (FABP4/aP2), CD36, and perilipin, reflecting the acquisition of functional adipocyte characteristics (Gregoire *et al*., 1998).

The process of adipogenesis is governed by a tightly regulated transcriptional cascade that is triggered upon MDI induction. The earliest transcription factors induced are CCAAT/enhancerbinding protein β (C/EBPβ) and CCAAT/enhancer-binding protein δ (C/EBPδ)**,** whose expression is stimulated by glucocorticoid and cyclic adenosine monophosphate (cAMP)-dependent signaling pathways. These early transcription factors activate the expression of CCAAT/enhancer-binding protein α (C/EBPα) and peroxisome proliferator-activated receptor gamma (PPARγ)**,** two master regulators that drive terminal adipocyte differentiation by promoting the expression of adipocytespecific genes involved in lipid metabolism, adipokine production, and insulin sensitivity (Cao *et al*., 1991; Tontonoz *et al*., 1994; Tontonoz *et al*., 1995; Brun *et al*., 1996; Rosen & Spiegelman, 2000).

The CCAAT/enhancer-binding protein (C/EBP) family comprises six members such as C/EBPα, C/EBPβ, C/EBPδ, C/EBPγ, C/EBPε, and C/EBPζ, all of which contain a conserved basic leucine zipper (bZIP) domain that enables DNA binding as well as homo- and heterodimerization (Vinson et al., 1989). Among these, *C/EBPα*, *C/EBPβ*, and *C/EBPδ* play central roles in adipogenesis. *C/EBPβ* and *C/EBPδ* function during the early phase of differentiation by inducing *C/EBPα* expression, whereas *C/EBPα* maintains the differentiated adipocyte phenotype by regulating genes involved in lipid metabolism, glucose homeostasis, and insulin responsiveness (Cao *et al*., 1991; Rosen & Spiegelman, 2000).

The indispensable roles of C/EBP transcription factors in adipogenesis have been demonstrated through both *in vitro* and *in vivo* studies. Loss of *C/EBPβ* or *C/EBPδ* impairs adipocyte differentiation and lipid accumulation, whereas ectopic expression of *C/EBPα* is sufficient to induce adipogenic conversion in appropriate cell systems (Freytag *et al*., 1994; Yeh *et al*., 1995). Similarly, mice deficient in *C/EBPβ* or *C/EBPδ* exhibit reduced adipose tissue development, while *C/EBPα*-deficient mice display severe defects in adipocyte differentiation, lipid storage, and adipocyte function (Wang *et al*., 1995; Flodby *et al*., 1996; Tanaka *et al*., 1997). These findings underscore the coordinated actions of *C/EBPβ*, *C/EBPδ*, and *C/EBPα* in establishing and maintaining the adipogenic program.

Collectively, adipogenesis is a highly regulated process that is essential for adipose tissue development and metabolic homeostasis. However, dysregulated adipocyte differentiation contributes to excessive white adipose tissue expansion, altered adipokine secretion, chronic lowgrade inflammation, and the development of obesity-associated metabolic disorders, including insulin resistance, type 2 diabetes mellitus, and cardiovascular disease (Hotamisligil *et al*., 1993; Di Rocco *et al*., 2024). Considering the pivotal roles of *C/EBPβ* and *C/EBPδ* in the initiation of adipogenesis, further investigation into the molecular mechanisms underlying their regulation may advance the development of targeted therapeutic approaches for obesity and obesity-associated metabolic diseases.

Chapter 2

Review of Literature

2.1 Adipogenesis

Adipogenesis is the process by which fibroblast-like preadipocytes differentiate into mature adipocytes (Rosen *et al*., 2000). Adipocytes originate from multipotent mesenchymal stem cells that, upon exposure to various signaling molecules, commit to the adipocyte lineage (Gregoire *et al*., 1998). This tightly regulated process involves the sequential differentiation of adipose-derived stem cells into preadipocytes, which subsequently mature into lipid-laden adipocytes (Sarantopoulos *et al*., 2018).

The primary function of adipocytes is to store triacylglycerol during periods of excess caloric intake and to mobilize these energy reserves when energy expenditure exceeds caloric intake. In addition, mature adipocytes possess the complete complement of enzymes and regulatory proteins required for both de novo lipogenesis and lipolysis (Cornelius *et al*., 1994).

2.2 Adipose Tissue: Types, Functions, and Metabolic Importance

Adipose tissue is an active endocrine organ that plays a central role in maintaining metabolic homeostasis. Its dysfunction or excessive accumulation is closely associated with obesity and related metabolic disorders (Ahmad *et al*., 2020). The global rise in obesity has intensified scientific interest in adipose tissue biology and adipogenesis, the process through which adipocytes are formed (Tang & Lane, 2012).

Based on their morphology and physiological functions, adipose tissue is classified into two major types: white adipose tissue (WAT) and brown adipose tissue (BAT) (Cannon & Nedergaard, 2004). WAT serves as the primary site of energy storage and functions as an endocrine organ by secreting adipokines and cytokines that regulate metabolic and inflammatory processes (Ouchi *et al*., 2011). In contrast, BAT is specialized for non-shivering thermogenesis, dissipating energy as heat through the action of mitochondrial uncoupling protein 1 (UCP1) (Kajimura *et al*., 2015).

In addition to WAT and BAT, beige (brite) adipocytes represent an inducible thermogenic adipocyte subtype that expresses UCP1 in response to specific physiological or environmental stimuli. Because of their capacity to increase energy expenditure, beige adipocytes have emerged as promising therapeutic targets for obesity and other metabolic disorders (De Paula *et al*., 2025). Although murine studies have provided important insights into the biology of thermogenic adipose tissue, the direct translation of these findings to humans remains challenging due to speciesspecific differences in adipose tissue distribution, abundance, and thermogenic capacity (De Paula *et al*., 2025).

2.3 Cellular Models Used to Study Adipogenesis

Multipotent stem cell lines and preadipocyte cell lines are extensively utilized to investigate adipogenesis, adipocyte proliferation, differentiation, and the secretion of adipokines. Adipogenesis is typically categorized into two sequential stages: commitment and terminal differentiation, both of which are governed by specific adipogenic signals (Smith *et al*., 1988).

Over the past two decades, the cellular and molecular mechanisms that underlie adipocyte development have been thoroughly examined using preadipocyte culture systems (Grégoire *et al*., 1998). Preadipocytes are found throughout adulthood, display depot-specific traits, and arise from various progenitor cell populations, where they undergo proliferation followed by differentiation into mature adipocytes (Sarantopoulos *et al*., 2018). Preadipocytes obtained from different animal models have been the subject of extensive research, with rodent-derived cells being the most commonly utilized, while feline and porcine cells have been used to a lesser degree (Rodriguez *et al*., 2004).

2.4 3T3-L1 Cell Line as an In Vitro Model of Adipogenesis

3T3-L1 cell line, established by Howard Green and colleagues (1974) from Swiss mouse 3T3 fibroblasts, is one of the most widely used *in vitro* models for studying adipogenesis, adipocytespecific gene expression, lipid metabolism, and metabolic regulation (Green & Kehinde, 1974; Smas & Sul, 1997). Owing to its high adipogenic potential and reproducible differentiation, the 3T3-L1 cell line has become a well-established model for investigating the molecular and cellular mechanisms underlying adipocyte development (Grégoire *et al*., 1998).

Adipogenic differentiation of 3T3-L1 cells is typically induced using the MDI cocktail, which rapidly activates immediate-early genes that initiate the adipogenic transcriptional program (Cornelius *et al*., 1994). During differentiation, the cells undergo coordinated morphological, biochemical, and transcriptional changes that drive their transition from fibroblast-like preadipocytes to mature adipocytes. These changes include the sequential activation of adipogenic genes and the progressive accumulation of intracellular lipid droplets, a hallmark of mature adipocytes (MacDougald & Lane, 1995; Rubin, 1978).

Approximately 24 hours after MDI induction, growth-arrested preadipocytes re-enter the cell cycle and undergo post-confluent mitosis**,** also known as mitotic clonal expansion, during which they complete at least one round of DNA replication and cell division (Bernlohr *et al*., 1985). Following this proliferative phase, the cells exit the cell cycle and enter a terminal growth-arrest state, which is essential for adipocyte differentiation (Scott *et al*., 1982). This transient mitotic event is thought to facilitate chromatin remodeling, thereby enabling adipogenic transcription factors to access regulatory elements of genes required for the mature adipocyte phenotype (Cornelius *et al*., 1994).

The importance of growth arrest in cellular differentiation has been demonstrated by several studies, which identified it as a prerequisite for terminal differentiation (Nadal-Ginard, 1978). Upon completion of differentiation, mature adipocytes accumulate large intracellular lipid droplets that serve as triglyceride storage depots and represent a defining feature of the adipocyte phenotype (Rizzatti *et al*., 2013).

2.5 Hormonal Regulation and Signaling Pathways in Adipogenesis

Adipocyte differentiation is a highly coordinated process regulated by a complex network of transcription factors, signaling pathways, and hormonal cues that direct the conversion of precursor cells into mature adipocytes (Rosen & Spiegelman, 2000). Early studies established that adipogenesis is tightly controlled by the interplay of hormonal, genetic, and environmental factors, with hormones such as insulin, glucocorticoids, and thyroid hormones playing pivotal roles in initiating and regulating adipogenic signaling pathways (Rosen *et al*., 2000).

In *in vitro* models, adipogenic differentiation is commonly induced using a combination of insulin, dexamethasone, and 3-isobutyl-1-methylxanthine (IBMX), collectively referred to as the MDI

cocktail (Grégoire *et al*., 1998). IBMX promotes adipogenesis by inhibiting phosphodiesterase activity, thereby increasing intracellular cyclic adenosine monophosphate (cAMP) levels (Student *et al*., 1980). Elevated cAMP activates cAMP response element-binding protein (CREB), which regulates the transcription of genes essential for adipocyte differentiation (Tang & Lane, 2012).

Insulin signaling is indispensable for adipogenesis, and disruption of this pathway impairs adipose tissue development and metabolic homeostasis (Blüher *et al*., 2002). Activation of insulin and insulin-like growth factor-1 (IGF-1) receptors stimulates downstream signaling molecules, including phosphatidylinositol 3-kinase (PI3K), protein kinase B (Akt1/2), and the mammalian target of rapamycin (mTOR), which collectively promote adipocyte differentiation, lipid accumulation, and metabolic maturation (Garofalo *et al*., 2003; Ali *et al*., 2013).

During the early stages of differentiation, growth-arrested preadipocytes undergo mitotic clonal expansion, a prerequisite for terminal adipocyte differentiation (MacDougald & Lane, 1995). This process is regulated by coordinated hormonal and extracellular signals that converge on adipogenic transcriptional networks, ultimately driving the formation of lipid-laden, functionally mature adipocytes (Ali *et al*., 2013).

2.6 Role of Early Adipogenic Transcription Factors

Adipocyte differentiation is primarily regulated through the sequential activation of transcription factors belonging to the CCAAT/enhancer-binding protein (C/EBP) and peroxisome proliferatoractivated receptor (PPAR) families (Siersbæk *et al*., 2010). Following adipogenic induction, preadipocytes undergo mitotic clonal expansion, during which the early adipogenic transcription factors *C/EBPβ* and *C/EBPδ* are rapidly induced (Hishida *et al*., 2009). These factors initiate the adipogenic transcriptional cascade by activating the expression of *PPARγ* and *C/EBPα*, the master regulators of terminal adipocyte differentiation (Erickson *et al*., 2001; Hishida *et al*., 2009). Together, *PPARγ* and *C/EBPα* coordinate the expression of adipocyte-specific genes required for the development, maturation, and maintenance of functional adipocytes (Siersbæk *et al*., 2010). In addition, insulin plays a pivotal role in adipogenesis by regulating the expression of *C/EBPα, C/EBPβ,* and *C/EBPδ*, thereby promoting the differentiation of preadipocytes into mature adipocytes (MacDougald *et al*., 1995).

2.7 Additional Transcriptional Regulators of Adipogenesis

Krüppel-like factors (KLFs) are important regulators of adipogenesis, functioning as either positive or negative modulators of adipocyte differentiation. *KLF6* and *KLF9* promote adipogenesis by enhancing the expression of peroxisome proliferator-activated receptor gamma (*PPARγ*), thereby facilitating adipocyte differentiation. In contrast, *KLF2* and *KLF7* suppress adipogenesis by downregulating *PPARγ* expression, thereby inhibiting the differentiation of preadipocytes into mature adipocytes (Pei *et al*., 2011).

Sterol regulatory element-binding protein 1c (SREBP1c) is another key pro-adipogenic transcription factor that promotes adipocyte differentiation by increasing the expression and transcriptional activity of *PPARγ* (Kim & Spiegelman, 1996; Kim *et al*., 1998). Conversely, several transcription factors, including GATA2, GATA3, Forkhead box O1 (FOXO1), and Forkhead box A2 (FOXA2), negatively regulate adipogenesis. GATA2 and GATA3 are highly expressed in preadipocytes but are progressively downregulated during adipocyte differentiation, indicating that their suppression is required for terminal adipocyte maturation (Tong *et al*., 2005).

(Ianiro *et al*., 2023) demonstrated that lactoferrin is an additional regulator of adipogenesis. Exogenous lactoferrin modulates adipocyte differentiation and improves insulin sensitivity in human adipocytes. Furthermore, lactoferrin expression changes during the differentiation of both human preadipocytes and 3T3-L1 cells and is regulated by adipogenic inducers such as rosiglitazone, suggesting its involvement in the regulation of adipogenesis.

2.8 MicroRNAs in Adipogenesis

MicroRNAs (miRNAs) are important post-transcriptional regulators of adipogenesis that modulate the expression of genes involved in adipocyte differentiation. Among these, miR-103, miR-107, and miR-143 are upregulated during adipocyte differentiation and contribute to adipogenesis. Overexpression of miR-103 and miR-143 enhances the differentiation of 3T3-L1 cells by promoting triglyceride accumulation and increasing the expression of adipocyte-specific genes (Xie *et al*., 2009).

2.9 Nrf2 Signalling in Adipogenesis

Nuclear factor erythroid 2-related factor 2 (Nrf2) is an important regulator of adipogenesis, although its role remains controversial. Pi *et al*., (2010) reported that Nrf2 promotes adipocyte differentiation, as Nrf2 deficiency reduced the expression of adipogenic transcription factors, including *PPARγ* and *C/EBPα*, whereas Keap1 knockdown enhanced adipogenesis. Similarly, Hou *et al*. (2020) demonstrated that Nrf2 regulates adipogenesis through *C/EBPβ* and is required for normal adipocyte differentiation. In contrast, Liu *et al*. (2023) showed that Nrf2 activation suppresses adipogenesis by reducing the expression of adipogenic markers, including *PPARγ*, *C/EBPα*, and fatty acid-binding protein 4 (FABP4), thereby inhibiting lipid accumulation. These findings suggest that the role of Nrf2 in adipogenesis is context-dependent and may vary according to cellular conditions and experimental models.

2.10 Clinical Significance and Future Perspectives

Adipocyte differentiation is essential for maintaining energy homeostasis, regulating lipid storage, and preserving insulin sensitivity. Dysregulation of adipogenesis contributes to the development of obesity, insulin resistance, type 2 diabetes, and other metabolic disorders. Therefore, understanding the molecular mechanisms underlying adipocyte differentiation is fundamental to elucidating adipose tissue biology and metabolic regulation.

Future research should focus on identifying the molecular pathways, signaling networks, and genetic and epigenetic mechanisms that regulate adipogenesis. Emerging areas such as epigenetic modifications, microRNA-mediated regulation, circadian rhythm, and redox signaling warrant further investigation because of their potential roles in adipose tissue development and metabolic homeostasis. Improved understanding of these regulatory mechanisms may facilitate the identification of novel therapeutic targets and support the development of personalized treatment strategies and regenerative medicine approaches for obesity and other metabolic diseases

Chapter 3

Aim and Objectives

Aim

The present study aims to investigate the gene expression pattern of *C/EBPβ* and *C/EBPδ* during adipocyte differentiation.

Objectives

- To induce adipocyte differentiation in 3T3-L1 cell model.
- To confirm adipocyte differentiation by morphological evaluation.
- To isolate total RNA and synthesize cDNA.
- To analyze the expression levels of *C/EBPβ* and *C/EBPδ* by qRT-PCR.

Chapter 4

Materials and Methods

4.1 Materials

4.1.1 Laboratory Materials

- T-25 tissue culture flasks
- 6-well tissue culture plates
- Cryovials
- Sterile centrifuge tubes (15 mL and 50 mL)
- Sterile microcentrifuge (Eppendorf) tubes
- Sterile micropipette tips
- Hemocytometer (Neubauer chamber)
- Coverslips
- Gel casting tray and comb
- Erlenmeyer flask
- PCR tubes
- Aluminium foil
- Syringe filter unit
- Disposable gloves and other laboratory consumables

4.1.2 Reagents for Cell Culture

- Dulbecco's Modified Eagle Medium (DMEM)
- Fetal bovine serum (FBS)
- Penicillin–streptomycin (1 %)
- Phosphate-buffered saline (PBS)
- 0.25 % Trypsin–EDTA solution
- Dimethyl sulfoxide (DMSO)
- Sodium bicarbonate ($NaHCO_3$)

4.1.3 Reagents for Cell Revival

- 70 % Ethanol
- Complete DMEM (DMEM supplemented with 10 % FBS and 1 % penicillin–streptomycin), pre-warmed to 37 °C

4.1.4 Reagents for Cryopreservation

- Freezing medium (complete DMEM containing 10 % DMSO)
- 70 % Ethanol

4.1.5 Reagents for Cell Counting

- Trypan blue solution (0.4 %)

4.1.6 Reagents for Cell Seeding

- Phosphate-buffered saline (PBS)
- 0.25 % Trypsin–EDTA solution
- Complete DMEM

4.1.7 Reagents for Adipocyte Differentiation

- MDI induction medium (3-isobutyl-1-methylxanthine [IBMX], dexamethasone, and insulin)
- Maintenance medium (DMEM supplemented with 10 % FBS)

4.1.8 Reagents for Oil Red O Staining

- Oil Red O working solution
- 4 % Paraformaldehyde (PFA) fixative
- 60 % Isopropanol

4.1.9 Reagents for RNA Isolation (TRIzol Method)

- TRIzol™ Reagent (Invitrogen™)
- Chloroform
- Isopropanol
- 75 % Ethanol (prepared using RNase-free water)
- RNase-free water or 0.1 % DEPC-treated water
- RNaseZap™ solution

4.1.10 Reagents for Agarose Gel Electrophoresis

- 1.2 % High-purity agarose
- DEPC-treated water
- 50× TAE buffer
- Ethidium bromide (EtBr) or an equivalent nucleic acid stain

4.1.11 Reagents for cDNA Synthesis and Quantitative Real-Time PCR (qRT-PCR)

- iScript™ cDNA Synthesis Kit (Bio-Rad Laboratories, USA)
- SYBR® Green Master Mix (Bio-Rad Laboratories, USA)
- Forward and reverse primers

4.1.12 Instruments

- Class II HEPA-filtered biosafety cabinet (ESCO Lifesciences, Singapore)
- CO_2 incubator (Eppendorf, Germany)
- Inverted phase-contrast microscope (Leica Microsystems, Germany)
- Refrigerated centrifuge (Eppendorf, Germany)
- Microcentrifuge (Eppendorf, Germany)
- Vortex mixer (Shimadzu, Japan)
- pH meter (Thermo Scientific, USA)
- Analytical balance (Shimadzu, Japan)

- Biophotometer (Eppendorf, Germany)
- Gel electrophoresis apparatus (Bio-Rad Laboratories, USA)
- Gel documentation system (Bio-Rad Laboratories, USA)
- Thermal cycler (Thermo Fisher Scientific, USA)
- Real-Time PCR Detection System (Bio-Rad Laboratories, USA)
- Water bath
- Refrigerator (4 °C)
- Deep freezers (−20 °C and −80 °C)
- Magnetic stirrer with hot plate
- Microwave oven

4.2 Methods

4.2.1 Cell Culture

3T3-L1 cell line was procured from National Centre for Cell Science (NCCS), Pune, India, and maintained according to standard cell culture procedures under aseptic conditions. Cells were cultured in high-glucose Dulbecco's Modified Eagle Medium (DMEM) supplemented with 10 % fetal bovine serum (FBS) and 1 % penicillin-streptomycin. Cells were maintained at 37 °C in a humidified incubator containing 5 % CO_2. Cell morphology and confluency were monitored regularly using an inverted phase-contrast microscope. Cells were subcultured upon reaching 70–80 % confluency to maintain optimal growth and prevent contact inhibition. For long-term storage, cells were cryopreserved in freezing medium containing 10 % DMSO to preserve cell viability and structural integrity.

4.2.2 Preparation of DMEM

Dulbecco's Modified Eagle Medium (DMEM) was prepared according to the manufacturer's instructions. Powdered DMEM was dissolved in approximately 900 mL of sterile distilled water with continuous stirring until completely dissolved. Sodium bicarbonate (3.7 g/L) was added, and the solution was mixed until clear. The final volume was adjusted to 1000 mL with sterile distilled water. The medium was sterilized using a 0.22 µm vacuum filtration system and collected in a sterile storage bottle. 10 % fetal bovine serum (FBS) and 1 % penicillin-streptomycin were added to prepare complete DMEM.

4.2.3 Subculture of 3T3-L1 Cells

Cells were subcultured when they reached approximately 70–80 % confluency to maintain healthy growth and optimal differentiation potential. The spent culture medium was aspirated from T-25 culture flasks, and the cell monolayer was gently rinsed twice with 1 mL sterile phosphate-buffered saline (PBS) to remove residual serum. Cells were then treated with an appropriate volume of Trypsin-EDTA and incubated at 37 °C for 2–5 minutes until detachment was observed. Complete DMEM was added to neutralize the trypsin, and the cell suspension was collected and centrifuged at 1000 rpm for 5 minutes. The resulting cell pellet was resuspended in fresh complete DMEM, and the cells were seeded into new culture flasks containing 5 ml of fresh media at the desired split ratio. The cells were further incubated at 37 °C in a humidified atmosphere containing 5 % CO_2.

4.2.4 Cell counting

The hemocytometer (Neubauer chamber) and coverslip were cleaned with 70 % ethanol, allowed to air dry, and the coverslip was carefully positioned over the counting chamber. A 10 µL aliquot of the cell suspension was loaded into the hemocytometer by gently dispensing the sample at the edge of the coverslip, allowing the chamber to fill by capillary action without introducing air bubbles or overfilling.

The hemocytometer was placed on an inverted phase-contrast microscope and examined under a 10× objective. Cells were counted within the four large corner squares of the Neubauer chamber, each consisting of 16 smaller squares. To avoid double counting, only cells touching the top and left boundary lines were included in the count, whereas cells touching the bottom and right boundary lines were excluded.

The total viable cell concentration was calculated using the following formula:

Total cells/mL = (Total cells counted × Dilution factor × 10^4) / Number of squares counted.

4.2.5 Cell seeding

Cells maintained in the T-25 culture flask were first examined under an inverted microscope to assess cell morphology and confluency. The spent culture medium was carefully discarded. The adherent cells were then washed twice with 1 mL of phosphate-buffered saline (PBS) to remove residual medium and dead cells. Approximately 400 µL of trypsin solution was added to the flask, and the cells were incubated for about 2 minutes to facilitate cell detachment. The detachment process was monitored microscopically to avoid over-trypsinization. After complete detachment, 1 mL of complete growth medium was added to neutralize the trypsin activity. The resulting cell suspension was collected and transferred into a sterile centrifuge tube. For cell counting, 10 µL of the cell suspension was loaded onto a hemocytometer with a coverslip. The total cell concentration was determined microscopically. Subsequently, the cells were seeded into a sterile 6-well tissue culture plate. Each well was seeded with an appropriate volume of the diluted cell suspension in complete growth medium to obtain a final cell density of 1×10^4– 2×10^4 cells per well. The plate was gently rocked in a horizontal and vertical direction to ensure uniform distribution of the cells. It was then labeled, sealed with Parafilm®, and incubated at 37 °C in a humidified incubator maintained at 5 % CO_2 for 48 hours**.**

4.2.6 Adipocyte differentiation

4.2.6.1 Induction Media Stock Solution Preparation

Stock solutions of 3-isobutyl-1-methylxanthine (IBMX), Dexamethasone and Insulin were prepared by dissolving each compound in Dimethyl sulfoxide (DMSO). For adipogenic induction, 18 mL of induction medium was required for a 6-well plate (3 mL per well). Therefore, 20 mL of induction medium was prepared to ensure sufficient volume. The final induction medium was prepared by supplementing DMEM base medium with 100 µL of 100 mM IBMX, 4 µL of 5 mM dexamethasone, and 20 µL of 10 mg/mL insulin per 20 mL total volume. This resulted in final working concentrations of 0.5 mM IBMX, 1 µM Dexamethasone, and 10 µg/mL Insulin in the induction medium.

4.2.6.2 Induction media treatment (Day 0)

The induction medium was formulated by supplementing DMEM base medium with 100 µL of 100 mM 3-isobutyl-1-methylxanthine (IBMX), 4 µL of 5 mM dexamethasone, and 20 µL of 10 mg/mL insulin. The final volume was adjusted to 20 mL. The 6-well plate containing seeded 3T3L1 preadipocytes was retrieved from the incubator, and the complete growth medium was aspirated and discarded under aseptic condition. Subsequently, 3 mL of freshly prepared MDI induction medium was added to each well to initiate adipogenic differentiation. The plate was then incubated at 37 °C in a 5 % CO_2 atmosphere for 48 hours. This time point was designated as Day 0 of differentiation.

4.2.6.3 Insulin treatment (Day 4)

The 6-well plate was monitored regularly under an inverted microscope to check the cell morphology and differentiation status. Following 4 days of MDI induction, the induction medium was aspirated from each well and discarded under aseptic conditions. The insulin medium was freshly prepared by supplementing DMEM containing 10 % FBS with insulin to a final concentration of 10 µg/mL. Specifically, 20 µL of 10 mg/mL insulin stock solution was added to 20 mL of DMEM + 10 % FBS. Subsequently, 3 mL of insulin medium was added to each well except first well (control well) and the media in the control well was replaced with DMEM supplemented with 10 % FBS. The plate was then incubated at 37 °C in a 5 % CO_2 atmosphere.

4.2.6.4 Maintenance Medium Renewal (Days 6, 8, and 10)

Following insulin treatment, the medium was replaced with maintenance medium every 48 hours to support adipocyte maturation. The 6-well plate was examined under an inverted microscope regularly to monitor lipid droplet accumulation. The insulin medium was aspirated from each well and discarded under aseptic conditions. Subsequently, 3 mL of maintenance medium, (10 % DMEM) was added to each well. The plate was then incubated at 37 °C, 5 % CO_2 incubator.

4.2.6.5 Collection of cells for RNA isolation (Day 2, 6 and 12)

After induction, the cell morphology was assessed by inverted microscopy. For RNA extraction, the culture medium was aspirated from one well, and cells were lysed directly by the addition of 1 mL of TRIzol® reagent.

Table 1. Work flow of 3T3-L1 cell differentiation

Day	Activity
Day 0	Induction media (100 ml of IBMX (0.5mM), 4µL of Dexamethasone (1µM) and 20 µL of insulin (10µg/ml) was added.
Day 2	Cells collected for RNA isolation.
Day 4	Induction media replaced with 10 % DMEM containing insulin (10 µg/ ml).
Day 6	Cells collected for RNA isolation and spent medium was replaced with 10 % DMEM.
Day 8 & 10	Media renewal (10 % DMEM).
Day 12	Cells collected for RNA isolation and Oil Red O Staining.

4.2.7 Oil Red O Staining

Following adipogenic differentiation, intracellular lipid accumulation in 3T3-L1 cells was assessed using Oil Red O staining according to the method described by Pittenger *et al*., (1999).

4.2.7.1 Preparation of Oil Red O Working Solution

The Oil Red O working solution was prepared immediately prior to use. Three parts of Oil Red O stock solution (0.5 % w/v in 100 % isopropanol) were mixed with two parts of distilled water. The solution was allowed to stand for 10 minutes and then filtered through Whatman No. 1 filter paper to remove precipitates.

4.2.7.2 Preparation of 4 % paraformaldehyde solution

4 % paraformaldehyde (PFA) solution was prepared in 1X phosphate-buffered saline (PBS, pH 7.4). 10 mL of 1X PBS was heated to 60 °C with constant stirring. Subsequently, 0.4 g of PFA powder was added gradually while stirring. To facilitate dissolution, 1 N NaOH was added drop wise until the solution became clear. After complete dissolution, the solution was cooled to room temperature and the pH was adjusted to 7.2–7.4 using 1 N HCl. The final volume was adjusted to 10 mL with 1X PBS.

4.2.7.3 Procedure:

The culture medium was aspirated, and cells were gently washed twice with 1X PBS. Subsequently, 2 mL of 4 % paraformaldehye (or 10 % neutral buffered formalin) was added to each well by pipetting onto the wall of the well to avoid cell detachment. The plate was incubated for 30–60 minutes. The paraformaldehye was discarded, and the cells were washed twice with distilled water. Cells were then incubated with 1 mL of 60 % v/v isopropanol per well for 5 minutes to facilitate Oil Red O penetration. The 60 % isopropanol was aspirated, and cells were covered evenly with 2 mL of freshly prepared Oil Red O working solution per well. The plate was incubated for 10–20 minutes with gentle rotation to ensure uniform staining. The Oil Red O solution was discarded, and the cells were washed 2–5 times with distilled water until no excess stain was visible in the wash solution. Cells were maintained in distilled water to prevent drying and were imaged using an inverted microscope.

4.2.8 RNA isolation by TRIzol Method

Before RNA isolation, the workbench, micropipettes, centrifuge, and all plastic wares were thoroughly decontaminated with RNaseZap (Ambion) to eliminate RNase contamination. All aqueous solutions were prepared using 0.1 % diethyl pyrocarbonate (DEPC; Sigma)-treated water. The solutions were incubated overnight at room temperature and subsequently autoclaved for 20 min to hydrolyze residual DEPC. All reagents used throughout the procedure were prepared with DEPC-treated water to ensure an RNase-free environment.

For total RNA isolation the cells were lysed and homogenized using TRIzol Reagent (Invitrogen) following the manufacturer's protocol. Initially, the culture medium was aspirated from the wells, and cells were lysed directly by the addition of 1 mL of TRIzol® reagent per well. The lysate was homogenized by pipetting and incubated for 5 minutes at room temperature to permit complete dissociation of nucleoprotein complexes. Chloroform (0.2 mL per 1 mL TRIzol®) was added to the homogenate. The tube was capped securely, shaken vigorously for 15 seconds, and incubated at room temperature for 2–3 minutes. The mixture was then centrifuged at 12,000 rpm for 15 minutes at 4 °C. Following centrifugation, the mixture separated into a lower red phenolchloroform phase, an interphase, and a colorless upper aqueous phase containing RNA. The aqueous phase was carefully transferred to a fresh microcentrifuge tube. RNA was precipitated by adding 0.5 mL of isopropanol per 1 mL TRIzol® used. The sample was incubated at room temperature for 10

minutes and centrifuged at 12,000 rpm for 10 minutes at 4 °C. The RNA pellet was visible as a gel-like precipitate at the bottom of the tube. The supernatant was discarded, and the RNA pellet was washed with 1 mL of 75 % ethanol (7.5 ml ethanol with 2.5 ml DEPC water) per 1 mL TRIzol® used. The sample was vortexed briefly and centrifuged at 2000 rpm for 4 minutes at 4 °C. The ethanol was discarded, and the RNA pellet was air-dried for 5–10 minutes. The RNA pellet was resuspended in 20–50 µL of RNase-free water by pipetting and incubated at 55–60 °C for 10 minutes. The purified RNA was immediately stored at −80 °C for subsequent cDNA synthesis and qPCR analysis.

4.2.9 Assessment of RNA Quality

4.2.9.1 RNA Purity

The purity of the isolated RNA was assessed using the absorbance ratios $A_{260/A280}$ and $A_{260/A230}$ measured using a biophotometer. RNA samples exhibiting $A_{260/A280}$ and $A_{260/A230}$ ratios approximately 2.0 were considered as pure and used for downstream applications such as cDNA synthesis and quantitative real-time PCR (qRT-PCR).

4.2.9.2 RNA integrity

The integrity of RNA was evaluated by agarose gel electrophoresis. The procedure is as follows.

Gel Preparation:

A 1.2 % agarose gel was prepared by dissolving 0.6 g of agarose powder in 50 mL of 1X TBE buffer prepared in DEPC-treated water and heated in a microwave until the agarose was completely dissolved. The gel solution was cooled to approximately 60 °C, and Eco Safe Nucleic Acid Staining Solution was added as per the manufacturer's instructions. The solution was poured into a gel casting tray, and a comb was inserted. The gel was allowed to solidify at room temperature for 30 minutes.

Sample Preparation:

Total RNA (1 µg) was mixed with 6X RNA loading dye.

Electrophoresis:

The solidified gel was placed in an electrophoresis tank containing 1X TAE running buffer prepared with DEPC-treated water. The RNA samples mixed with 6X RNA loading dye and a molecular marker were loaded into the wells. Electrophoresis was performed at 80 V for 45–60 minutes until the tracking dye had migrated approximately 75 % of the gel length.

Visualization:

The gel was visualized using a gel documentation system. RNA integrity was confirmed by the presence of distinct 28S and 18S ribosomal RNA bands with an intensity ratio of approximately 2:1.

4.2.10 cDNA Synthesis iScript™ cDNA Synthesis Kit (Bio-Rad Laboratories, USA) is used for two-step reverse transcription quantitative PCR (qRT-PCR).

Reaction set up:

Table 2: Reaction mixture used for cDNA synthesis

Component	Volume per reaction (µL)
5x iscript Reaction Mix	4 µL
iscript Reverse Transcriptase	1 µL
RNA template	5 µL
Nuclease-free water	10 µL
Total volume	**20 µL**

The reaction condition for cDNA synthesis is as follows:

Table 3: Thermal cycling conditions for cDNA synthesis

Reaction	Temperature	Time
Priming	25 °C	5 min
Reverse transcription	46 °C	20 min
RT inactivation	95 °C	1 min
Optional step	Hold at 4 °C	

4.2.11 Primer Dilution

The lyophilized forward and reverse primers were procured commercially and diluted using nuclease free water. The lyophilized primer was briefly centrifuged to collect the contents from the bottom of the tube. Nuclease-free water was added according to the manufacturer's datasheet to obtain a final stock solution concentration of 100 µM (100 pmol/µL). The solution was vortexed and briefly centrifuged. A 10 µM (10 pmol/µL) of working solution was prepared by diluting 10 µL of the stock solution with 90 µL of nuclease-free water. The working solution was vortexed and stored at −20°C until further use in qPCR analysis.

Table 4: Primer sequence used for qRT-PCR

Sl No	Gene Symbol	Gene Name	Primer Sequence	Reference
1.	*C/EBPβ*	CCAAT/enhancer-binding protein beta	Forward – 5'-GCAAGAGCCGCGACAAG-3' Reverse – 5'-GGCTCGGGCAGCTGCTT-3'	Yamaguchi *et al*., (2017)
2.	*C/EBPδ*	CCAAT/enhancer binding protein delta	Forward – 5'-TCGACTTCAGCGCCTACATTGACT-3' Reverse- 5'-CCGCTTTGTGGTTGCTGTTGAAGA-3'	Yamaguchi *et al*., (2017)
3.	*GAPDH*	Glyceraldehyde-3-phosphate dehydrogenase	Forward – 5'-ACTCCACTCACGGCAAATTC-3' Reverse – 5'-TCTCCATGGTGGTGAAGACA-3'	Xie *et al*., (2025)

4.2.12 Quantitative Real-time PCR (qRT-PCR)

Differential expression of *C/EBPβ* and *C/EBPδ* was evaluated using quantitative real-time PCR (qRT-PCR). RNA extracted from differentiated and control cells were reverse-transcribed to cDNA, and 1 µL cDNA was used as the template for each reaction. *GAPDH* served as the endogenous control in all the experiments. Reactions were performed in triplicates with a total

volume of 10 µL, and a non-template control (NTC) was included in each run to monitor contamination.

Table 5: Reaction mixture used for qRT-PCR

Components	Volume per reaction (µL)
SYBR® Green Supermix (2x)	5 µL
Forward primer	1 µL
Reverse primer	1 µL
Nuclease-free water	2 µL
cDNA template	1 µL
Total volume	10 µL

4.2.12.1 Thermal Cycling Protocol

The real-time PCR instrument was programmed with the specified thermal cycling protocol, and the PCR tubes containing the reaction mixture were placed into the instrument for amplification. Upon completion of the run, the amplification data were analyzed according to the manufacturer's instrument-specific guidelines.

Table 6: Thermal cycling conditions for qRT-PCR (40 cycles)

Reaction	Temperature	Time
Initial denaturation	95 °C	2-3 min
Denaturation	98 °C	15 sec
Annealing / Extension plate read	60 °C	30 sec

Melt curve analysis was conducted at the end of each run to verify the specificity of amplification.

4.2.12.2 Data Analysis

The relative gene expression levels of target genes were calculated using $2^{(-\Delta\Delta Ct)}$ Method (Livak and Schmittgen, 2001). *GAPDH* was used as the endogenous reference gene (housekeeping gene) for normalization. All reactions were performed as triplicates and mean Ct values were used for further analysis. Data were expressed as mean ± standard error. Fold changes in gene expression were calculated by comparing the Ct values of 2^{nd}, 6^{th},12^{th} day samples with control Sample.

Relative fold change was calculated by the equation:

$$\Delta Ct = Ct\ (Target\ gene) - Ct\ (Reference\ Gene)$$

$$\Delta\Delta Ct = \Delta Ct\ (Test) - \Delta Ct\ (control)$$

$$Fold\ change = 2^{(-\Delta\Delta Ct)}$$

Chapter 5

Results

5.1 Morphology of 3T3-L1 Preadipocytes

Under undifferentiated culture conditions, 3T3-L1 preadipocytes exhibited the characteristic fibroblast-like, spindle-shaped morphology typical of proliferating preadipocytes (Fig. 4). The cells appeared elongated with well-defined cytoplasmic extensions and formed a uniform, adherent monolayer and no visible intracellular lipid droplets were detected, confirming their undifferentiated state prior to the induction of adipogenic differentiation.

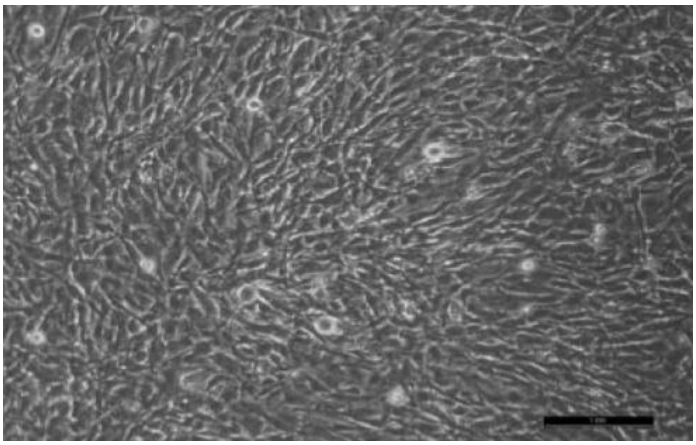


Figure 4: Microscopic image showing the morphology of undifferentiated 3T3-L1 cells

5.1.1 Morphological changes and lipid droplet accumulation in 3T3-L1 cells during adipocyte differentiation

Preadipocytes were treated with an MDI cocktail to induce their differentiation into mature adipocytes. During the differentiation process, the fibroblast-like (spindle-shaped) preadipocytes gradually changed their morphology, became rounded in shape, and progressively accumulated intracellular lipid droplets (Fig. 5a- Fig. 5e) that increased in both size and number, ultimately resulting in the formation of rounded, lipid-rich mature adipocytes.

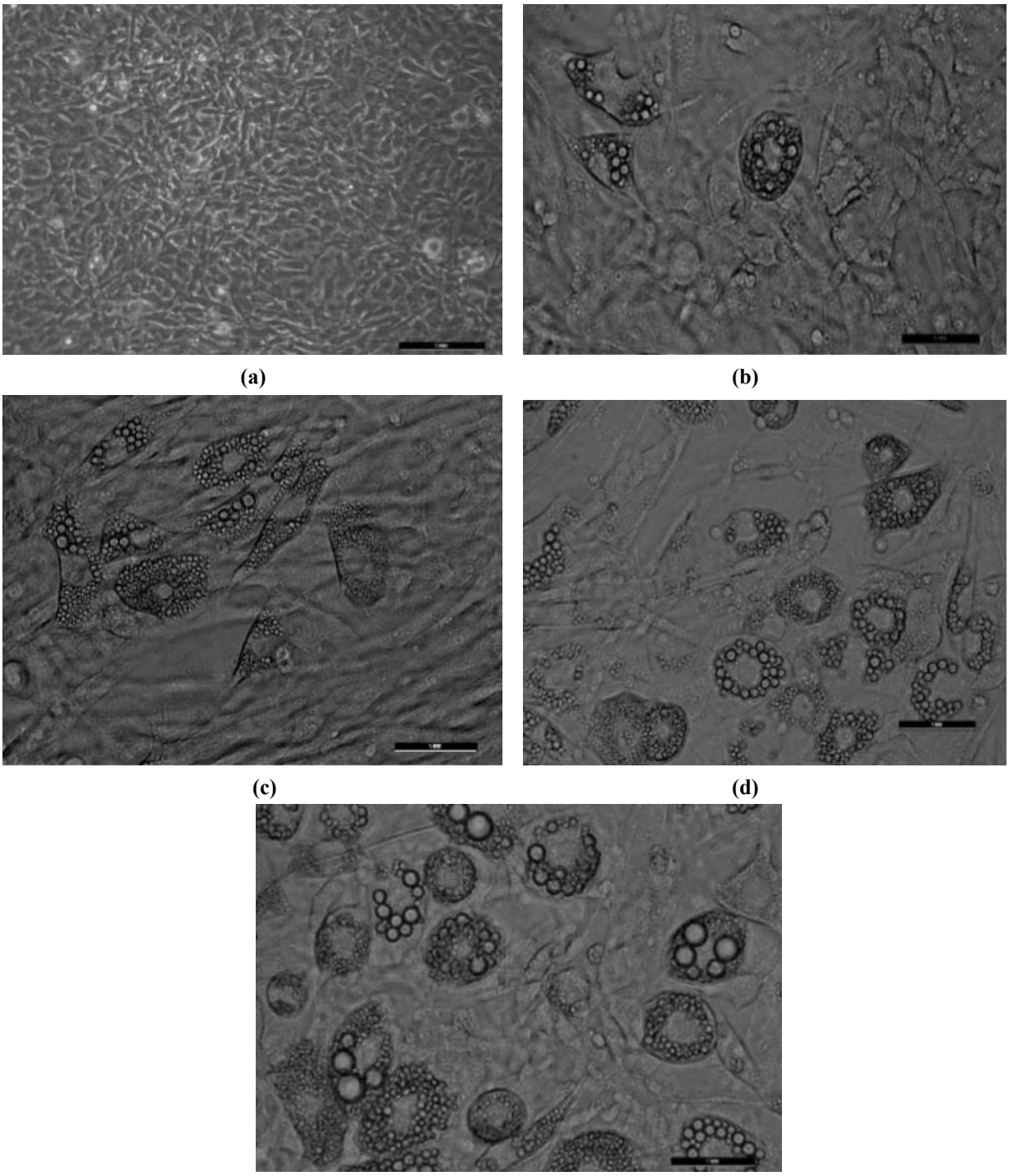


Figure 5: Microscopic images showing the progressive accumulation of lipid droplets in 3T3-L1 cells during the course of adipocyte differentiation. (a)- Day 2, (b) - Day 4, (c) - Day 6, (d) - Day 8 and (e) - Day 12

5.1.2 Oil Red O Staining

Adipocyte differentiation was confirmed by Oil Red O staining. At Day 2, negligible amount of intracellular lipid droplets were present, which increased in size on Day 4 (Fig. 6a)and Day 8 (Fig. 6b), reaching even more ORO-positive lipid droplets on Day 12 (Fig. 6c). The increase in intracellular lipid droplet accumulation was clearly visible throughout the differentiation process (Fig. 7).

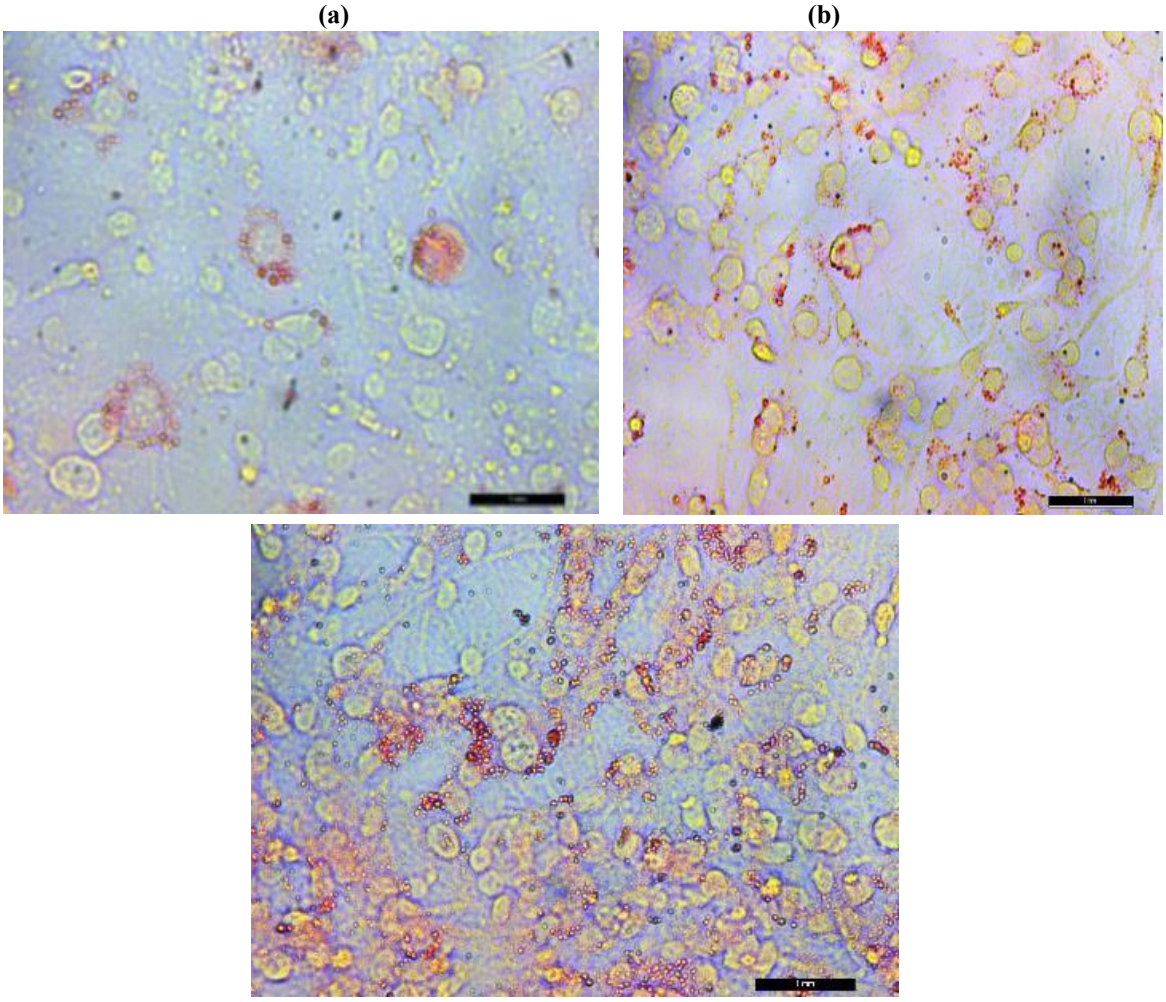
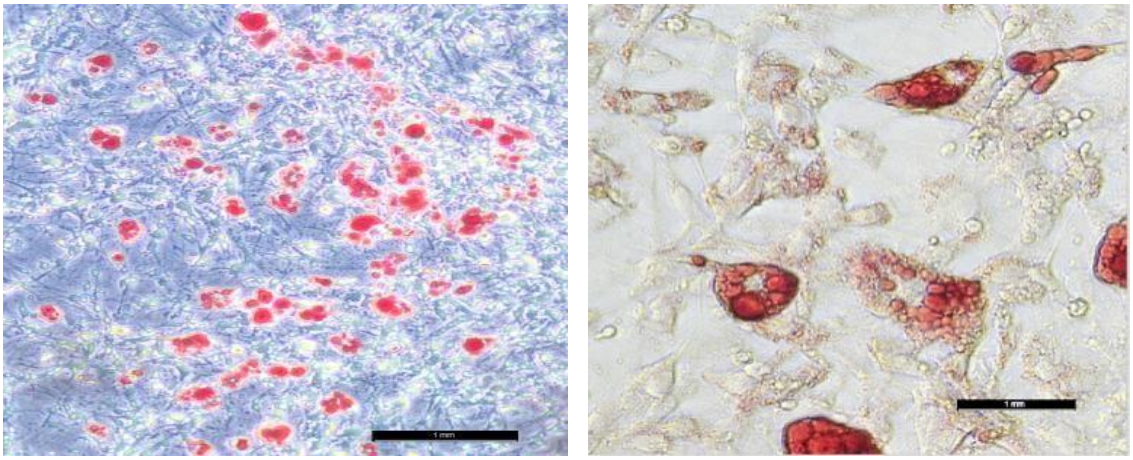


Figure 6: Microscopic images of Oil Red O-stained 3T3-L1 cells during adipogenic differentiation showing the progressive accumulation of intracellular lipid droplets at 20× magnification. Images were captured on (a) Day 4, (b) Day 8, and (c) Day 12 following the induction of differentiation



(a) **(b)**

Figure 7: Representative images of Oil Red O Staining of differentiated 3T3-L1 cells. (a)10x magnification, (b) 40x magnification

5.2 Total RNA analysis

5.2.1 Assessment of concentration and purity by biophotometric analysis

The purity and concentration of RNA was assessed by biophotometric analysis. The A_{260}/A_{280} and A_{260}/A_{230} absorbance ratio of all samples was approximately 2, indicating good quality RNA with minimal contamination (Table 7).

Table 7: Biophotometric data analysis of RNA quality

Sample	Concentration (ng/µl)	A_{260}/A_{280}	A_{260}/A_{230}
Preadipocyte	273.24	1.95	1.88
2	623.84	1.99	1.89
6	251.10	1.98	1.91
12	321.64	2.00	1.92

5.2.2 Assessment of RNA Integrity by Agarose Gel Electrophoresis

The integrity of the isolated total RNA was assessed by 1.2 % agarose gel electrophoresis. Two distinct ribosomal RNA (rRNA) bands corresponding to the 28S and 18S rRNA were observed in all samples (Fig. 8). The 28S rRNA band appeared more intense than the 18S rRNA band,

indicating that the RNA remained intact with minimal degradation. No smearing was observed, confirming the high quality and integrity of the isolated RNA.

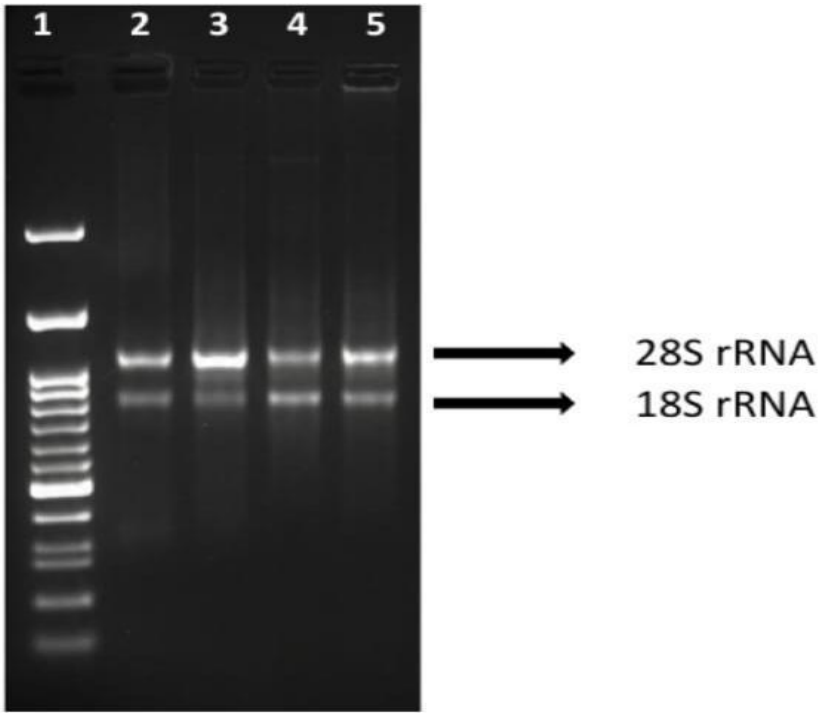


Figure 8: Total RNA isolated from cells at various stages of differentiation
Lane 1: 100 bp DNA ladder; Lane 2: RNA from preadipocytes (3T3-L1); Lane 3: RNA from the cells at 2nd day of differentiation; Lane 4: RNA from the cells at 6th day of differentiation; Lane 5: RNA from the cells at 12th day of differentiation

5.3 cDNA quality assessment

To evaluate the quality and synthesis efficiency of the cDNA, qPCR was performed using primers specific to the glyceraldehyde 3-phosphate dehydrogenase (*GAPDH*) housekeeping gene and was used as the endogenous control in all the experiments. Amplification of *GAPDH* yielded highly reproducible results with low quantification cycle values, indicating substantial and consistent template abundance across samples, confirming its suitability for downstream gene expression analysis (Fig. 9).

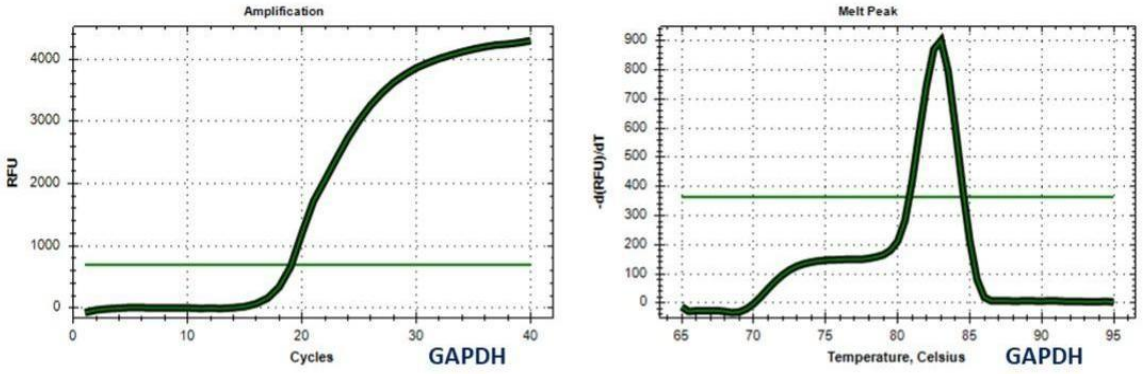


Figure 9: Representative qPCR amplification and melt curve analysis of the *GAPDH* reference gene used for cDNA quality assessment

5.3.1 qPCR Amplification Curve Analysis

The quantitative real-time PCR (qPCR) amplification curves exhibited the characteristic sigmoidal profile expected for efficient target amplification. Each amplification plot initially displayed a stable baseline phase, during which the fluorescence signal remained at background levels due to the absence of detectable PCR product accumulation. This was followed by a distinct exponential phase, characterized by a rapid increase in fluorescence intensity as the target nucleic acid was amplified with high efficiency. Subsequently, the amplification curves entered a linear transition phase before reaching a plateau phase, where the fluorescence signal stabilized as amplification efficiency declined because of reagent depletion, accumulation of PCR products, and reduced enzyme activity. The observed amplification profiles indicated successful amplification of the target genes and demonstrated the reliability and efficiency of the qPCR assay. A representative amplification curve demonstrating efficient qPCR amplification is represented in Fig. 10.

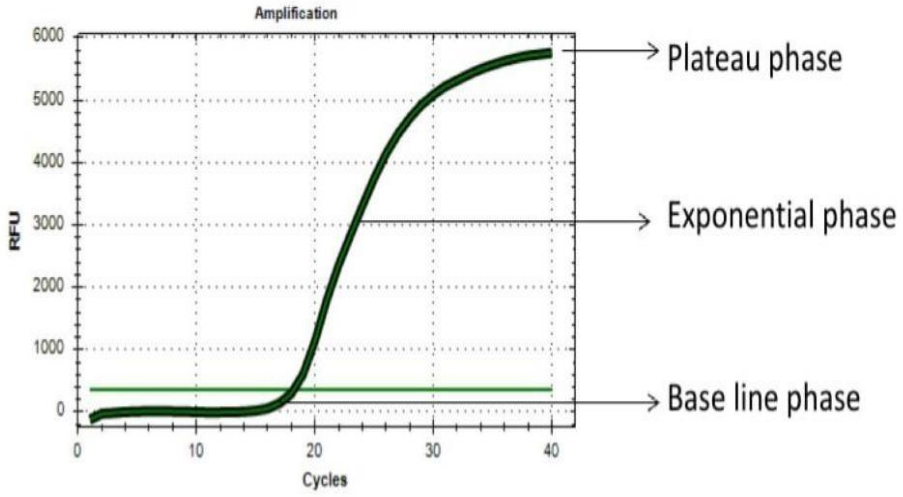


Figure 10: Representative amplification curve demonstrating efficient qPCR amplification, characterized by an early quantification followed by a strong exponential phase

5.3.2 qPCR Melt Curve Analysis

Melt curve analysis further confirmed the high specificity of the reaction, characterized by a single sharp melt peak indicating specific amplification of the target gene with no significant primerdimer formation or non-specific PCR products (Fig. 11).

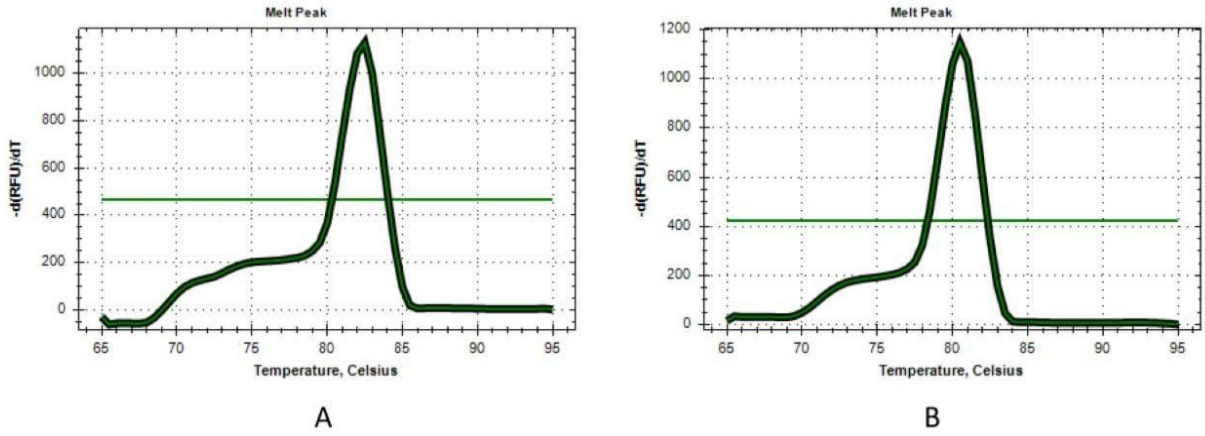


Figure 11: Melt curve analysis: Single, sharp melt peak showing accurate amplification (A) *C/EBPβ*; (B) *C/EBPδ*

5.4 Relative expression analysis of *C/EBPβ*

The relative expression of *C/EBPβ* gene was quantified by quantitative real-time PCR (qPCR) using the $2^{-(\Delta\Delta Ct)}$ method. Gene expression levels were expressed as fold changes relative to the undifferentiated control, which was normalized to a value of 1. The fold change analysis demonstrated differential expression of *C/EBPβ* among samples collected on 2nd day, 6th day and 12th day of adipogenic differentiation. The expression of *C/EBPβ* was found upregulated immediately upon adipogenic induction (day 2) followed by day 6, and then gradually decreased by day 12. The quantitative results are summarized in Table 8 and illustrated in Figure 12.

Table 8: Relative expression of the *C/EBPβ* gene during adipogenesis, quantified by qPCR using the $2^{-(\Delta\Delta Ct)}$ method.

Day	Fold change $= 2^{-(\Delta\Delta Ct)}$
Day 2	0.81
Day 6	0.92
Day 12	0.43

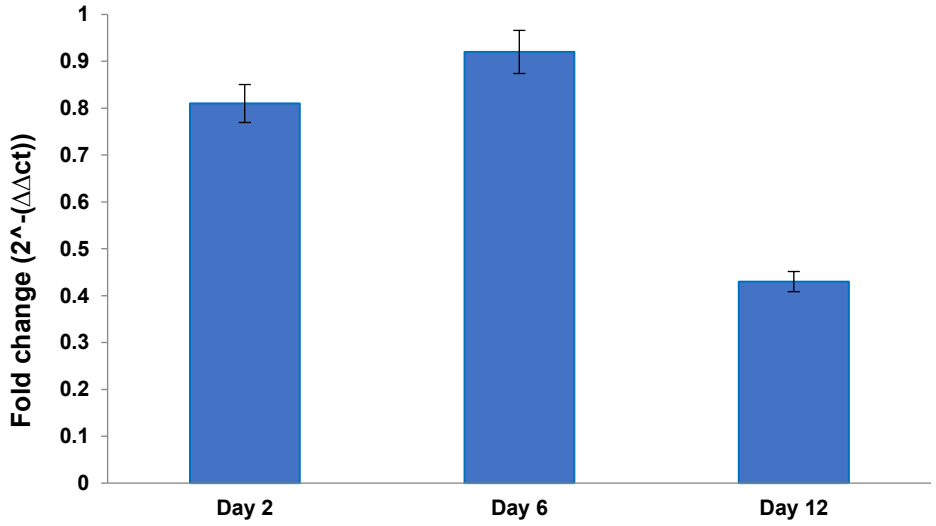


Figure 12: Relative fold change in *C/EBPβ* gene expression during adipogenic differentiation at Day 2, Day 6 and Day 12.

5.5 Relative expression analysis of *C/EBPδ*

The relative expression of the *C/EBPδ* gene was quantified by quantitative real-time PCR (qPCR) using the $2^{-(\Delta\Delta Ct)}$ method. Gene expression levels were expressed as fold changes relative to the undifferentiated cells. The fold change analysis demonstrated differential *C/EBPδ* expression on 2nd day, 6th day and 12th day. *C/EBPδ* also followed a similar expression pattern to that of *C/EBPβ*, showing a comparable temporal trend with peak expression at the intermediate stage followed by a decline during the later stage of differentiation. The expression of *C/EBPδ* was increased to 1.69-fold on day 6, and sharply declined to 0.15-fold by day 12, indicating the role of *C/EBPδ* as an early adipogenic transcription factor. The results are presented in Table 9 and Figure 13.

Table 9: Relative expression of the *C/EBPδ* gene during adipogenesis, quantified by qPCR using the $2^{-(\Delta\Delta Ct)}$ method

Day	Fold change $= 2^{-(\Delta\Delta Ct)}$
Day 2	0.85
Day 6	1.69
Day 12	0.15

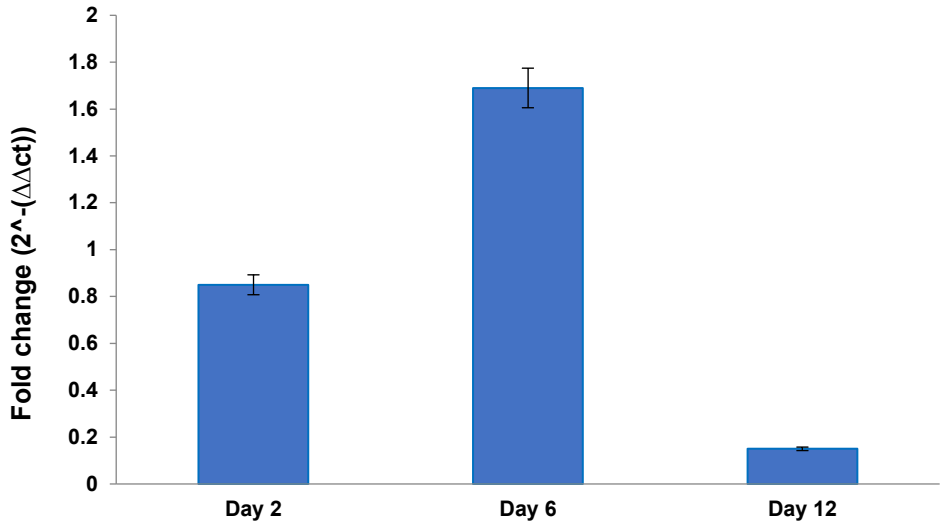


Figure 13: Relative fold change in *C/EBPδ* gene expression during adipogenic differentiation at Day 2, Day 6 and Day 12

Chapter 6

Discussion

In the present study, adipocyte differentiation was successfully induced in 3T3-L1 preadipocytes using a standard adipogenic induction cocktail containing insulin, dexamethasone, and IBMX. Following induction, the cells underwent a characteristic morphological transition from fibroblastlike preadipocytes to rounded adipocytes with intracellular lipid droplet accumulation, confirming successful adipogenic differentiation (Green and Kehinde, 1975; Zebisch *et al*., 2012).

The initiation of adipocyte differentiation was accompanied by the rapid induction of the early transcription factors *C/EBPβ* and *C/EBPδ* (Cao *et al*., 1991; Farmer, 2006). IBMX increased intracellular cAMP levels by inhibiting phosphodiesterase activity, thereby activating protein kinase A (PKA) signaling and promoting the expression of *C/EBPβ* (Tang & Lane, 2012; Rosen & MacDougald, 2006). Dexamethasone activated glucocorticoid signaling, leading to the induction of *C/EBPδ* during the early stage of adipogenesis (Rosen & MacDougald, 2006; Farmer, 2006). Both transcription factors were transiently expressed during the early phase of adipocyte differentiation and functioned as essential regulators of adipogenesis (Cao *et al*., 1991; Farmer, 2006).

The qPCR analysis performed in the present study demonstrated differential expression of *C/EBPβ* and *C/EBPδ* during adipocyte differentiation. *C/EBPβ* exhibited higher expression during the early stage of differentiation, consistent with its role as an immediate early-response transcription factor following adipogenic induction (Cao *et al*., 1991; Rosen & MacDougald, 2006). *C/EBPδ* also followed a similar expression pattern to that of *C/EBPβ*, showing a comparable temporal trend with peak expression at the intermediate stage followed by a decline during the later stage of differentiation. These early transcription factors act cooperatively to initiate the adipogenic cascade by activating downstream regulators such as *PPARγ* and *C/EBPα*, thereby committing cells to terminal adipocyte differentiation (Farmer, 2006). Therefore, the observed higher early expression of *C/EBPδ* compared with *C/EBPβ* is consistent with its role as a rapidly inducible glucocorticoid-responsive gene during the initiation of adipogenesis. The transient expression pattern observed for both genes suggests that their primary functions were restricted to the early stages of adipocyte differentiation (Cao *et al*., 1991; Rosen & MacDougald, 2006).

Overall, the expression profiles obtained in the present study support the established roles of *C/EBPβ* and *C/EBPδ* as early regulators of adipocyte differentiation. The observed temporal expression patterns are consistent with their function as immediate early transcription factors that initiate the adipogenic program, leading to activation of downstream regulators such as *PPARγ* and *C/EBPα*. The transient nature of their expression further indicates their involvement in the early commitment phase of differentiation. Future studies involving detailed time-course analysis and functional validation are required to further clarify their regulatory roles during adipogenesis.

Summary and Conclusion

In the present study, adipogenic differentiation was successfully induced in 3T3-L1 preadipocytes using a standard induction cocktail comprising insulin, dexamethasone, and IBMX. Morphological observations confirmed successful differentiation, as the cells underwent a distinct phenotypic transition from fibroblast-like preadipocytes to rounded adipocytes characterized by the progressive accumulation of intracellular lipid droplets, a hallmark of adipocyte maturation.

The early phase of differentiation was marked by the rapid induction of the transcription factors *C/EBPβ* and *C/EBPδ*, both of which are recognized as key regulators of the adipogenic program. qPCR analysis demonstrated dynamic and time-dependent changes in their expression profiles, with both genes exhibiting transient upregulation during the initial stages of differentiation. This early induction reflects their role as immediate early response genes, activated in response to adipogenic stimuli. However, as differentiation progressed, the expression levels of both *C/EBPβ* and *C/EBPδ* declined during the later stages, indicating that their regulatory activity is largely restricted to the early commitment phase rather than terminal adipocyte maturation.

Overall, the findings suggest that *C/EBPβ* and *C/EBPδ* play a coordinated and time-sensitive role in initiating the adipogenic transcriptional cascade. Their early activation likely contributes to the subsequent induction of downstream master regulators such as *PPARγ* and *C/EBPα*, which drive terminal differentiation and lipid accumulation. The observed decline in expression during later stages further supports their function as early stage regulatory factors whose activity diminishes once the adipogenic program is fully established.

References

Ahmad, B., Serpell, C. J., Fong, I. L., & Wong, E. H. (2020). Molecular mechanisms of adipogenesis: The anti-adipogenic role of AMP-activated protein kinase. *Frontiers in Molecular Biosciences, 7*, 76.

Ali, A. T., Hochfeld, W. E., Myburgh, R., & Pepper, M. S. (2013). Adipocyte and adipogenesis. *European Journal of Cell Biology, 92*(6–7), 229–236.

Bernlohr, D. A., Bolanowski, M. A., Kelly, T. J., Jr., & Lane, M. D. (1985). Evidence for an increase in transcription of specific mRNAs during differentiation of 3T3-L1 preadipocytes. *Journal of Biological Chemistry, 260*(9), 5563–5567.

Blüher, M., Michael, M. D., Peroni, O. D., Ueki, K., Carter, N., Kahn, B. B., & Kahn, C. R. (2002). Adipose tissue-selective insulin receptor knockout protects against obesity and obesityrelated glucose intolerance. *Developmental Cell, 3*(1), 25–38

Bora, P., & Majumdar, A. S. (2017). Adipose tissue-derived stromal vascular fraction in regenerative medicine: A brief review on biology and translation. *Stem Cell Research & Therapy, 8*(1), 145.

Brun, R. P., Kim, J. B., Hu, E., Altiok, S., & Spiegelman, B. M. (1996). Adipocyte differentiation: a transcriptional regulatory cascade. *Current opinion in cell biology*, *8*(6), 826-832.

Cannon, B., & Nedergaard, J. (2004). Brown adipose tissue: Function and physiological significance. *Physiological Reviews, 84*(1), 277–359. Cao, Z., Umek, R. M., & McKnight, S. L. (1991). Regulated expression of three C/EBP isoforms during adipose conversion of 3T3-L1 cells. *Genes & development*, *5*(9), 1538-1552.

Cao, Z., Umek, R. M., & McKnight, S. L. (1991). Regulated expression of three C/EBP isoforms during adipose conversion of 3T3-L1 cells. *Genes & development*, *5*(9), 1538-1552.

Chularojmontri, L., Nanna, U., & Kaewamatawong, R. (2022). Inhibitory Effect of Carallia Brachiata Extract Through Regulation of Adipogenesis Pathways in 3T3-L1 Cells. *Pharmacognosy Journal*, *14*(5), 655-660.

Cornelius, P., Enerbäck, S., Bjursell, G., Olivecrona, T., & Pekala, P. H. (1988). Regulation of lipoprotein lipase mRNA content in 3T3-L1 cells by tumour necrosis factor. *Biochemical Journal, 249*(3), 765–769.

Cornelius, P., MacDougald, O. A., & Lane, M. D. (1994). Regulation of adipocyte development. *Annual Review of Nutrition, 14*(1), 99–129.

Cristancho, A. G., & Lazar, M. A. (2011). Forming functional fat: A growing understanding of adipocyte differentiation. *Nature Reviews Molecular Cell Biology, 12*(11), 722–734.

Dani, C., Amri, E. Z., Bertrand, B., Enerbäck, S., Bjursell, G., Grimaldi, P., & Ailhaud, G. (1990). Expression and regulation of pOb24 and lipoprotein lipase genes during adipose conversion. *Journal of Cellular Biochemistry, 43*(2), 103–110.

De Paula, A. D. S., Lorrany, G., Correia Garcia, E., Teles Soares Beserra, B., & Amorim Amato, A. (2025). Thermogenic differentiation of human adipocyte precursors in culture: A systematic review. *Cells, 14*(23), Article 1904.

Di Rocco, G., Trivisonno, A., Trivisonno, G., & Toietta, G. (2024). Dissecting human adipose tissue heterogeneity using single-cell omics technologies. *Stem Cell Research & Therapy, 15*(1), 322.

Erickson, R. L., Hemati, N., Ross, S. E., & MacDougald, O. A. (2001). P300 coactivates the adipogenic transcription factor CCAAT/enhancer-binding protein α. *Journal of Biological Chemistry, 276*(19), 16348–16355.

Farmer, S. R. (2006). Transcriptional control of adipocyte formation. *Cell metabolism*, *4*(4), 263273.

Fitzgerald, S. J., Janorkar, A. V., Barnes, A., & Maranon, R. O. (2018). A new approach to study the sex differences in adipose tissue. *Journal of biomedical science*, *25*(1), 89.

Flodby, P., Barlow, C., Kylefjord, H., Åhrlund-Richter, L., & Xanthopoulos, K. G. (1996). Increased hepatic cell proliferation and lung abnormalities in mice deficient in CCAAT/enhancer-binding protein α. *Journal of Biological Chemistry, 271*(40), 24753–24760.

Freytag, S. O., Paielli, D. L., & Gilbert, J. D. (1994). Ectopic expression of the CCAAT/enhancerbinding protein α promotes the adipogenic program in a variety of mouse fibroblastic cells. *Genes & Development, 8*(14), 1654–1663.

Garofalo, R. S., Orena, S. J., Rafidi, K., Torchia, A. J., Stock, J. L., Hildebrandt, A. L., ... Coleman, K. G. (2003). Severe diabetes, age-dependent loss of adipose tissue, and mild growth deficiency in mice lacking Akt2/PKBβ. *The Journal of Clinical Investigation, 112*(2), 197–208.

Gregoire, F. M. (2001). Adipocyte differentiation: From fibroblast to endocrine cell. *Experimental Biology and Medicine, 226*(11), 997–1002.

Gregoire, F. M., Smas, C. M., & Sul, H. S. (1998). Understanding adipocyte differentiation. *Physiological Reviews, 78*(3), 783–809.

Green, H., & Kehinde, O. (1974). Sublines of mouse 3T3 cells that accumulate lipid. *Cell, 1*(3), 113–116.

Green, H., & Kehinde, O. (1975). An established preadipose cell line and its differentiation in culture. II. Factors affecting the adipose conversion. *Cell, 5*(1), 19–27.

Hishida, T., Nishizuka, M., Osada, S., & Imagawa, M. (2009). The role of C/EBPδ in the early stages of adipogenesis. *Biochimie, 91*(5), 654–657. https://doi.org/10.1016/j.biochi.2009.01.007

Hotamisligil, G. S., Shargill, N. S., & Spiegelman, B. M. (1993). Adipose expression of tumor necrosis factor-α: Direct role in obesity-linked insulin resistance. *Science, 259*(5091), 87–91.

Hou, W., Chen, Q., Wang, H., Qiu, P., Lyu, X., Chen, W., ... Wang, R. (2020). The metabolic footprint during adipocyte commitment highlights ceramide modulation as an adequate approach for obesity treatment. *EBioMedicine, 51*, 102631.

Ianiro, G., Niro, A., Rosa, L., Valenti, P., Musci, G., & Cutone, A. (2023). To boost or to reset: the role of lactoferrin in energy metabolism. *International Journal of Molecular Sciences*, *24*(21), 15925.

Kajimura, S., Spiegelman, B. M., & Seale, P. (2015). Brown and beige fat: Physiological roles beyond heat generation. *Cell Metabolism, 22*(4), 546–559.

Kershaw, E. E., & Flier, J. S. (2004). Adipose tissue as an endocrine organ. *The Journal of Clinical Endocrinology & Metabolism, 89*(6), 2548–2556.

Kim, J. B., Sarraf, P., Wright, M., Yao, K. M., Mueller, E., Solanes, G., ... Spiegelman, B. M. (1998). Nutritional and insulin regulation of fatty acid synthetase and leptin gene expression through ADD1/SREBP1. *The Journal of Clinical Investigation, 101*(1), 1–9.

Kim, J. B., & Spiegelman, B. M. (1996). ADD1/SREBP1 promotes adipocyte differentiation and gene expression linked to fatty acid metabolism. *Genes & Development, 10*(9), 1096–1107.

Liu, Z., Deng, P., Liu, S., Bian, Y., Xu, Y., Zhang, Q., ... Pi, J. (2023). Is nuclear factor erythroid 2-related factor 2 a target for the intervention of cytokine storms? *Antioxidants, 12*(1), 172.

Livak, K. J., & Schmittgen, T. D. (2001). Analysis of relative gene expression data using real-time quantitative PCR and the $2^{-\Delta\Delta CT}$ method. *methods*, *25*(4), 402-408.

MacDougald, O. A., Hwang, C. S., Fan, H., & Lane, M. D. (1995). Regulated expression of the obese gene product (leptin) in white adipose tissue and 3T3-L1 adipocytes. *Proceedings of the National Academy of Sciences of the United States of America, 92*(20), 9034–9037.

MacDougald, O. A., & Lane, M. D. (1995). Transcriptional regulation of gene expression during adipocyte differentiation. *Annual Review of Biochemistry, 64*, 345–373.

Moller, D. E., & Flier, J. S. (1991). Insulin resistance—Mechanisms, syndromes, and implications. *The New England Journal of Medicine, 325*(13), 938–948.

Nadal-Ginard, B. (1978). Commitment, fusion and biochemical differentiation of a myogenic cell line in the absence of DNA synthesis. *Cell*, *15*(3), 855-864.

Novikoff, A. B., Novikoff, P. M., Rosen, O. M., & Rubin, C. S. (1980). Organelle relationships in cultured 3T3-L1 preadipocytes. *The Journal of Cell Biology, 87*(1), 180–196.

Ouchi, N., Parker, J. L., Lugus, J. J., & Walsh, K. (2011). Adipokines in inflammation and metabolic disease. *Nature reviews immunology*, *11*(2), 85-97.

Pei, H., Yao, Y., Yang, Y., Liao, K., & Wu, J. R. (2011). Krüppel-like factor KLF9 regulates PPARγ transactivation at the middle stage of adipogenesis. *Cell Death & Differentiation*, *18*(2), 315-327.

Pi, J., Leung, L., Xue, P., Wang, W., Hou, Y., Liu, D., ... Chan, J. Y. (2010). Deficiency in the nuclear factor E2-related factor 2 transcription factor results in impaired adipogenesis and protects against diet-induced obesity. *Journal of Biological Chemistry, 285*(12), 9292–9300.

Pittenger, M. F., Mackay, A. M., Beck, S. C., Jaiswal, R. K., Douglas, R., Mosca, J. D., ... & Marshak, D. R. (1999). Multilineage potential of adult human mesenchymal stem cells. *science*, *284*(5411), 143-147.

Rodriguez, A. M., Elabd, C., Delteil, F., Astier, J., Vernochet, C., Saint-Marc, P., ... Ailhaud, G. (2004). Adipocyte differentiation of multipotent cells established from human adipose tissue. *Biochemical and Biophysical Research Communications, 315*(2), 255–263.

Rizzatti, V., Boschi, F., Pedrotti, M., Zoico, E., Sbarbati, A., & Zamboni, M. (2013). Lipid droplets characterization in adipocyte differentiated 3T3-L1 cells: Size and optical density distribution. *European Journal of Histochemistry, 57*(3), e24.

Rosen, E. D., & MacDougald, O. A. (2006). Adipocyte differentiation from the inside out. *Nature Reviews Molecular Cell Biology, 7*(12), 885–896. https://doi.org/10.1038/nrm2066

Rosen, E. D., & Spiegelman, B. M. (2000). Molecular regulation of adipogenesis. *Annual Review of Cell and Developmental Biology, 16*, 145–171.

Rosen, E. D., & Spiegelman, B. M. (2014). What we talk about when we talk about fat. *Cell, 156*(1–2), 20–44.

Rosen, E. D., Walkey, C. J., Puigserver, P., & Spiegelman, B. M. (2000). Transcriptional regulation of adipogenesis. *Genes & Development, 14*(11), 1293–1307.

Rubin, C. S. (1978). Development of hormone receptors and hormonal responsiveness *in vitro*: Insulin receptors and insulin sensitivity in the preadipocyte and adipocyte forms of 3T3L1 cells. *Journal of Biological Chemistry, 253*, 7570–7578.

Sarantopoulos, C. N., Banyard, D. A., Ziegler, M. E., Sun, B., Shaterian, A., & Widgerow, A. D. (2018). Elucidating the preadipocyte and its role in adipocyte formation: A comprehensive review. *Stem Cell Reviews and Reports, 14*(1), 27–42.

Scott, R. E., Florine, D. L., Wille, J. J., Jr., & Yun, K. (1982). Coupling of growth arrest and differentiation at a distinct state in the G1 phase of the cell cycle: GD. *Proceedings of the National Academy of Sciences of the United States of America, 79*(3), 845–849.

Selvarajan, S., Lund, L. R., Takeuchi, T., Craik, C. S., & Werb, Z. (2001). A plasma kallikreindependent plasminogen cascade required for adipocyte differentiation. *Nature Cell Biology, 3*(3), 267–272.

Sharma, S., Muthu, S., Jeyaraman, M., Ranjan, R., & Jha, S. K. (2021). Translational products of adipose tissue-derived mesenchymal stem cells: Bench to bedside applications. *World journal of stem cells*, *13*(10), 1360.

Siersbæk, R., Nielsen, R., & Mandrup, S. (2010). PPARγ in adipocyte differentiation and metabolism: Novel insights from genome-wide studies. *FEBS Letters, 584*(15), 3242–3249.

Smas, C. M., & Sul, H. S. (1997). Molecular mechanisms of adipocyte differentiation and inhibitory action of pref-1. *Critical Reviews™ in Eukaryotic Gene Expression*, *7*(4).

Smith, P. J., Wise, L. S., Berkowitz, R., Wan, C., & Rubin, C. S. (1988). Insulin-like growth factorI is an essential regulator of the differentiation of 3T3-L1 adipocytes. *Journal of Biological Chemistry, 263*(19), 9402–9408.

Student, A. K., Hsu, R. Y., & Lane, M. D. (1980). Induction of fatty acid synthetase synthesis in differentiating 3T3-L1 preadipocytes. *Journal of Biological Chemistry, 255*(10), 4745–4750.

Tanaka, T., Yoshida, N., Kishimoto, T., & Akira, S. (1997). Defective adipocyte differentiation in mice lacking the C/EBPβ and/or C/EBPδ gene. *The EMBO Journal, 16*(24), 7432–7443.

Tang, Q. Q., & Lane, M. D. (2012). Adipogenesis: From stem cell to adipocyte. *Annual Review of Biochemistry, 81*, 715–736.

Tong, Q., Tsai, J., Tan, G., Dalgin, G., & Hotamisligil, G. S. (2005). Interaction between GATA and the C/EBP family of transcription factors is critical in GATA-mediated suppression of adipocyte differentiation. *Molecular and Cellular Biology, 25*(2), 706–715.

Tontonoz, P., Hu, E., & Spiegelman, B. M. (1994). Stimulation of adipogenesis in fibroblasts by PPARγ2, a lipid-activated transcription factor. *Cell, 79*(7), 1147–1156.

Tontonoz, P., Hu, E., & Spiegelman, B. M. (1995). Regulation of adipocyte gene expression and differentiation by peroxisome proliferator activated receptor γ. *Current opinion in genetics & development*, *5*(5), 571-576.

Vinson, C. R., Sigler, P. B., & McKnight, S. L. (1989). Scissors-grip model for DNA recognition by a family of leucine zipper proteins. *Science, 246*(4932), 911–916.

Wang, N. D., Finegold, M. J., Bradley, A., Ou, C. N., Abdelsayed, S. V., Wilde, M. D., Taylor, L. R., Wilson, D. R., & Darlington, G. J. (1995). Impaired energy homeostasis in C/EBPα knockout mice. *Science, 269*(5227), 1108–1112.

Wu, J., Boström, P., Sparks, L. M., Ye, L., Choi, J. H., Giang, A. H., ... & Spiegelman, B. M. (2012). Beige adipocytes are a distinct type of thermogenic fat cell in mouse and human. *Cell*, *150*(2), 366-376.

Xie, H., Lim, B., & Lodish, H. F. (2009). MicroRNAs induced during adipogenesis that accelerate fat cell development are downregulated in obesity. *Diabetes, 58*(5), 1050–1057.

Xie, B., Li, F., Yan, J., Cheng, M., & Hui, F. (2025). Polo-like kinase 2 ameliorates lipopolysaccharide-induced cardiac injury by blocking cardiomyocyte ferroptosis. *American Journal of Hypertension*, *38*(11), 938-946.

Yamaguchi, J., Tanaka, T., Saito, H., Nomura, S., Aburatani, H., Waki, H., ... Nangaku, M. (2017). Echinomycin inhibits adipogenesis in 3T3-L1 cells in a HIF-independent manner. *Scientific Reports, 7*(1), 6516.

Ye, R. Z., Richard, G., Gévry, N., Tchernof, A., & Carpentier, A. C. (2022). Fat cell size: Measurement methods, pathophysiological origins, and relationships with metabolic dysregulations. *Endocrine Reviews, 43*(1), 35–60.

Yeh, W. C., Cao, Z., Classon, M., & McKnight, S. L. (1995). Cascade regulation of terminal adipocyte differentiation by three members of the C/EBP family of leucine zipper proteins. *Genes & Development, 9*(2), 168–181.

Zebisch, K., Voigt, V., Wabitsch, M., & Brandsch, M. (2012). Protocol for cell culture, differentiation, and isolation of 3T3-L1 adipocytes. *Methods in Molecular Biology, 824*, 143–148.